

# Mechanism of the Heterogeneous Reaction of Hydrogen Chloride with Chlorine Nitrate and Hypochlorous Acid on Water Ice

Andrew B. Horn\*

Department of Chemistry, University of York, Heslington, York, YO1 5DD, U.K.

John R. Sodeau,\* Tristan B. Roddis, and Neil A. Williams

School of Chemical Sciences, University of East Anglia, Norwich, NR4 7TJ, U.K.

Received: September 22, 1997; In Final Form: May 14, 1998

The interactions of HOCl and ClONO<sub>2</sub> with pure and HCl-doped water ice have been reinvestigated using infrared spectroscopy in conjunction with static and thermal desorption mass spectrometry in the temperature range 140–180 K to probe the detailed mechanisms of their heterogeneous atmospheric reactions. In agreement with earlier studies, HOCl was found to react with hydroxonium chloride species to directly produce molecular chlorine. This molecular chlorine desorbed from the surface above ca. 155 K either directly or in subsequent thermal desorption experiments, depending upon substrate temperature at the time of reaction. ClONO<sub>2</sub> was observed to heterogeneously hydrolyze upon water ice to produce HOCl and hydrated H<sub>3</sub>O<sup>+</sup>NO<sub>3</sub><sup>-</sup>. Below ca. 155 K, HOCl remains adsorbed on the ice surface, while above ca. 155 K, it desorbs directly into the gas phase. These results suggest that a long-lived, adsorbed state of HOCl is unlikely to play a direct role in heterogeneous chemistry at stratospheric temperatures. The direct reaction of ClONO<sub>2</sub> with an ice surface saturated with ionic hydrates of HCl was observed to result in the production of molecular chlorine, which, as for the HOCl reaction, either remained adsorbed or desorbed from the surface depending upon temperature. This provides convincing evidence for the direct heterogeneous reaction of Cl<sup>-</sup> with ClONO<sub>2</sub> under stratospheric conditions. A novel explanation for the enhanced reactivity of ClONO<sub>2</sub> toward atmospherically relevant substrates is presented, in which a partially ionized precursor state is formed. Partial ionization of ClONO<sub>2</sub> along the Cl–O bond serves to increase the electrophilicity of the chlorine atom, making the site highly prone to nucleophilic attack by either water or adsorbed chloride ions.

## Introduction

The chemistry of the stratosphere, particularly in relation to the processes that control levels of ozone, has been studied intensively in recent years.<sup>1,2</sup> As a result of this activity, a wide body of data is available from both field measurements<sup>3</sup> and modeling studies<sup>4</sup> to support the hypothesis that heterogeneous processing involving atmospheric particles plays a major role in controlling the partitioning of atmospheric halogen species.<sup>5,6</sup> For example, the heterogeneous reactions of HOCl and ClONO<sub>2</sub> with HCl upon the surface of polar stratospheric clouds (PSCs)<sup>7</sup> and sulfate aerosols (SAs)<sup>8</sup> adequately account for discrepancies between model predictions based entirely upon gas-phase chemistry and field observations. The nature of the particulate material present in the stratosphere has also received a considerable amount of attention. Field studies over a wide range of atmospheric regions indicate the particles are predominantly aqueous solutions of sulfuric, nitric, and hydrochloric acid hydrates, which may be either solid or liquid depending upon temperature and relative humidity.<sup>9–11</sup> This is supported by the results of recent laboratory measurements and theoretical modeling studies.<sup>12–17</sup> The principal reactants that play a role in heterogeneous chemistry in the stratosphere are the oxides of nitrogen (such as NO<sub>2</sub>, NO<sub>3</sub>, and N<sub>2</sub>O<sub>5</sub>), the chlorine reservoir species ClONO<sub>2</sub>, HOCl, and HCl, and the particles themselves, containing sulfate and nitrate ions along with varying amounts of water. The distribution of the gaseous reactants is reasonably well understood from a wide range of field measurement

campaigns in recent years, providing an increasing database of the atmospheric concentrations of many of the important species.<sup>6,18</sup>

On the basis of these observations and deductions, numerous laboratory studies have attempted to recreate the conditions that occur in the atmosphere and to measure the rates and mechanisms of the reactions of the important species upon surfaces or aerosols that mimic atmospheric particles. These data have enabled current atmospheric models to attain a remarkable degree of accuracy. Experimental methods by which reaction rates are obtained from extended liquid surfaces include a variety of wetted wall flow tube techniques<sup>19–22</sup> or Knudsen cells.<sup>23,24</sup> However, as pointed out by Hanson, Ravishankara, and Solomon,<sup>25</sup> the existence of liquid particles leads to the possibility of surface/bulk diffusion, resulting in limited uptake and surface reactivity by particles where mobilities are high. Although corrections for small particle effects can be made, direct measurements upon aerosols and entrained droplets are becoming more commonplace. Appropriately sized and well-characterized particles can therefore be created and studied by a number of experimental methods, well documented in the literature.<sup>26–30</sup>

The characterization of atmospheric substrate mimics by vibrational spectroscopy has also proved exceptionally informative, with techniques such as reflection–absorption infrared spectroscopy on ultrathin condensed films being used with great success to study in detail the types of hydrates formed from

nitric and sulfuric acid in various ratios over a range of relevant temperatures.<sup>31–35</sup> Recent advances in instrumentation have also permitted the direct observation of aerosols by infrared spectroscopy, often in systems where temperature, pressure, and relative humidity can be varied to obtain realistic particle composition and phase information.<sup>36–40</sup> For example, using a low-temperature flowing aerosol cell, Clapp et al.<sup>41</sup> have recently reported a study of the freezing characteristics of the sulfuric acid/water system, in which they observe extreme supercooling of sulfate aerosols under realistic stratospheric conditions.

Laboratory-based spectroscopic studies of the interaction of atmospheric species with particle mimics have also yielded the most convincing chemical mechanisms by which heterogeneous reactions occur. The advantage of infrared spectroscopy is that it provides a direct method of observing and, more importantly, discriminating between different surface-adsorbed species. These species may be either adsorbed reactants or surface-bound reaction products. By following reactions through vibrational spectra while controlling experimental parameters such as reactant partial pressure, ambient and substrate temperature, and relative humidity, it has proved possible to obtain much of the information needed to construct detailed mechanisms for many atmospheric reactions, in many cases augmenting or verifying mechanistic assumptions deduced from indirect kinetic techniques. It is now also reasonably well established that heterogeneous processes occurring upon the atmospheric particle surfaces are dominated by chemical reaction mechanisms that are largely ionic in nature.<sup>42,43</sup> Kinetic measurements indicate that reaction efficiency is strongly correlated with the amount of water present in the particle or available at the reaction interface.<sup>44–46</sup> This feature, observed on substrates ranging from pure ice to ternary mixtures of sulfuric, nitric, and hydrochloric acid, highlights the fundamental role of heterogeneous hydrolysis and aqueous solvation in the chemistry of ozone depletion and explains the correlation observed in the field between ozone depletion, temperature, and relative humidity. The interaction of HCl with atmospheric particle surfaces provides a good example of the importance of aqueous solvation. Although some authors believe that they have detected molecular HCl under stratospheric conditions,<sup>47,48</sup> the majority of experimental evidence accumulated over recent years clearly demonstrates that, at all temperatures above 50 K, hydrogen chloride is readily hydrolyzed by water-rich particles to give ionic hydrates of the form  $\text{H}_3\text{O}^+(\text{H}_2\text{O})_n \cdot \text{Cl}^-$ .<sup>49–55</sup> The thermodynamics of adsorption and ionization have also been investigated theoretically,<sup>56–58</sup> from which similar conclusions as to the ionic nature of the adsorbate can be drawn. It is clear therefore from these studies that it is predominantly the chloride ion that participates in the heterogeneous atmospheric chemistry of HCl in water-rich environments.

Using accumulated data from a range of infrared studies, supported by kinetic evidence, we have suggested that a coherent nucleophile/electrophile reaction mechanism involving adsorption, ionization, and hydrolysis can be invoked to explain the reactivity and product distributions when highly polar materials such as  $\text{ClONO}_2$ ,  $\text{N}_2\text{O}_5$ , and HCl interact with ice surfaces.<sup>43</sup> Infrared spectroscopic studies suggest that the hydrolysis of  $\text{ClONO}_2$  is initiated by cleavage of the Cl–O bond to produce an adsorbed  $[\text{H}_2\text{OCl}]^+$  moiety and a nitrate ion. The subsequent (temperature-dependent) hydrolysis then yields the observed reaction products. Such a scheme also provides an explanation of certain trends observed in kinetic studies, as discussed by Rossi and co-workers,<sup>59</sup> where a short time delay is observed before the ejection of the reaction product HOCl from the

surface because of competition between the adsorbed ionic intermediate species and newly arriving  $\text{ClONO}_2$  for the available surface water. However, further experimental evidence is required to verify this mechanism and to probe the nature of the nucleophilic and electrophilic centers involved. Rossi and co-workers have also concluded, like ourselves, that the competition between adsorbed nucleophiles such as  $\text{H}_2\text{O}$  and  $\text{Cl}^-$  will determine the product branching ratios.<sup>59</sup>

In this paper, we report new, combined infrared spectroscopic and mass spectrometric studies of the  $\text{ClONO}_2/\text{HCl}/\text{H}_2\text{O}$  system which are designed to remove some of the existing controversies concerning the nature and identity of surface-located and desorbing species during the adsorption and reaction of  $\text{ClONO}_2$  on ice and HCl-doped ice surfaces. These controversies include the suggested requirement for  $\text{Cl}^-$  ions at the reacting surface, the effect of nitrate poisoning upon the surface reactivity, and the role (if any) of the postulated  $[\text{H}_2\text{OCl}]^+$  species. We have monitored the gas-phase composition above an ice surface and have obtained the infrared spectra of adsorbed species simultaneously, with the aim of accounting for all the species present during reaction. These observations support our mechanism for reaction processes at water-rich interfaces and provide strong evidence for the importance of polarization and partial ionization in the control of ice surface reaction mechanisms.

## Experimental Section

The experimental apparatus used in this study is based upon a modified version of custom-built apparatus described elsewhere.<sup>62</sup> An ultrahigh-vacuum chamber, pumped by an oil-vapor diffusion pump, is coupled to a BioRad FTS 60A/896 FTIR spectrometer. The sample substrate consists of a  $1 \times 2$  cm gold foil (0.25 mm thickness) welded to two 0.5 mm diameter tungsten supports. These supports are in thermal contact with a liquid nitrogen reservoir and also serve as electrical connections for resistively heating the substrate. Temperatures are measured using a chromel/alumel thermocouple junction, spot welded to the back of the gold foil. Because of the good thermal properties of gold, thermal gradients across the substrate are negligible. All chemical species were admitted into the vacuum chamber through independent glass dosing lines which are directed at the substrate surface from a distance of 25 mm to prevent cross-contamination of gases prior to their reaching the reaction surface and to minimize exposure to any other parts of the vacuum chamber. Pressure measurements were made using an uncalibrated cold-cathode ion gauge located behind the sample. Uncertainties in the measurement of gas fluxes at the sample due to sticking are estimated to be quite large, and quoted pressures should be used only as a guide. Mass spectrometric measurements were made using a differentially pumped triple-filter instrument of quadrupole design (Hiden Analytical, U.K.), facing the reaction substrate at a distance of ca. 25 mm. With an effective dynamic range in excess of 7 orders of magnitude, we are able to monitor the ejection of species such as HOCl and  $\text{Cl}_2$  from an ice surface during dosing and in the presence of a large excess of reactants. Under computer control, ionization and acceleration potentials were adjusted to obtain optimum yields of parent ions or fragments in regions of the  $m/e$  scale where maximum discrimination was possible. This is particularly important when trying to discriminate between species such as  $\text{ClONO}_2$  and HOCl, which give many of the same ionized fragments. For example, since they both yield  $^{35}\text{Cl}^{16}\text{O}^+$  fragments with  $m/e$  51, HOCl was typically measured as the parent ion,  $^1\text{H}^{16}\text{O}^{35}\text{Cl}^+$ , while  $\text{ClONO}_2$  was readily detected using its  $^{14}\text{N}^{16}\text{O}_2^+$  fragment

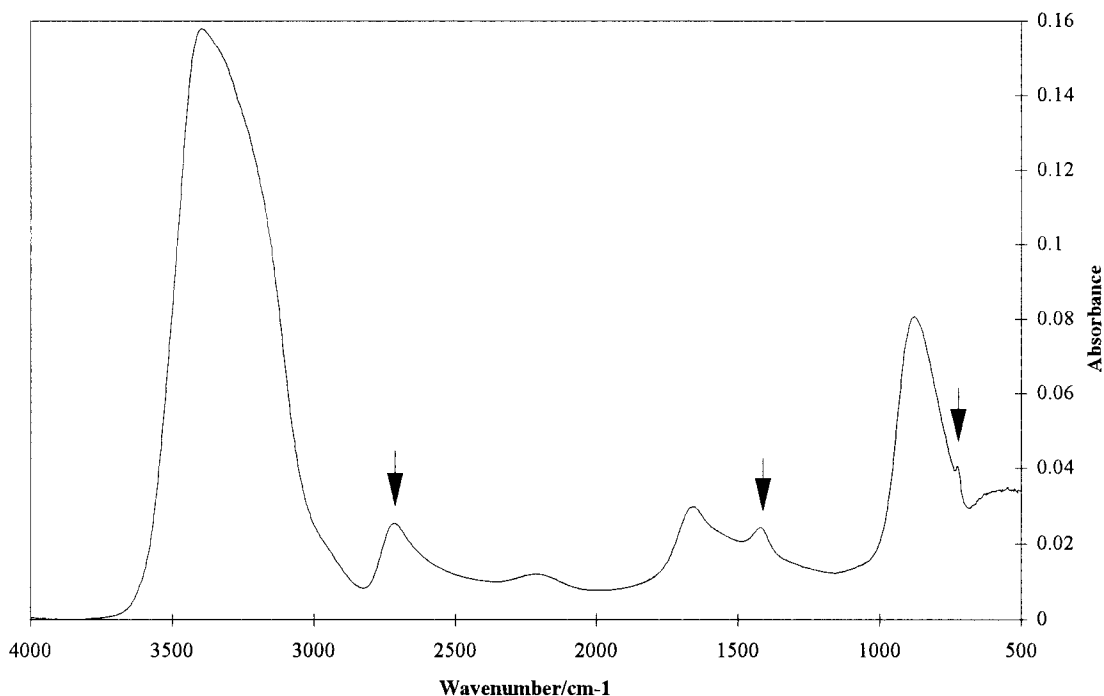


**Figure 1.** RAIR spectrum of HOCl adsorbed on ice at 145 K. Bands at 2716, 1421, and 725  $\text{cm}^{-1}$  (arrows) are readily assigned to molecular HOCl (see text).

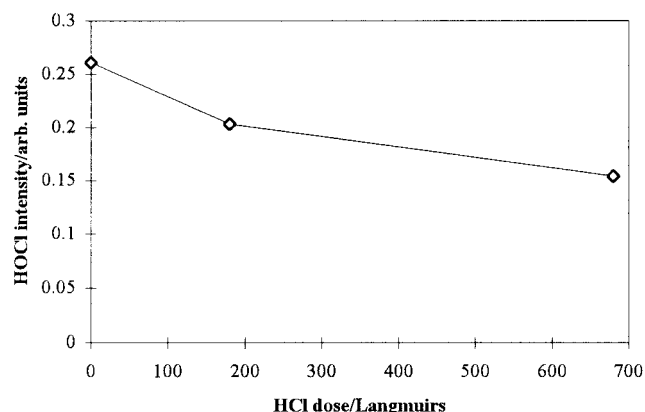


**Figure 2.** Integrated intensity of the  $\nu\text{OH}$  band of an adsorbed HOCl layer as a function of HCl dose at 140 K.

at  $m/e$  46 (the parent ion is usually quite weak). As a result, the relative fragment intensities observed in many cases differ from those cited in the literature.<sup>59</sup> A simple estimate of mass spectrometric sensitivity can be obtained from the data in Figure 5. The upper trace represents the  $^{35}\text{Cl}^+$  signal during exposure of the ice surface to  $3 \times 10^{-7}$  mbar HCl, which gives rise to ca.  $3 \times 10^6$  counts per second at the detector. Assuming linearity, a partial pressure of  $1 \times 10^{-13} \approx 1$  count per second. As a rough approximation, a gas at a pressure of  $1 \times 10^{-6}$  mbar produces a monolayer in ca. 1 s; hence the desorption of 1 monolayer in 100 seconds would result in a partial pressure of ca.  $1 \times 10^{-8}$  mbar during the desorption. Despite the crudeness of this calculation, we conservatively estimate our base sensitivity to be at least 0.1% of a monolayer for most species studied here. Thermal desorption spectra were obtained using a linear heating rate of ca.  $1 \text{ K s}^{-1}$ . Multiple ion traces were obtained using 100 ms dwell and collect times on each ion signal, giving a linear time-base resolution of ca. 1 s. RAIR spectra were recorded at a resolution of  $4 \text{ cm}^{-1}$  from the coaddition of 256 double-sided interferograms.

Reactant gases were either purchased in lecture bottles (HCl,  $\text{NO}_2$ ,  $\text{Cl}_2$ ) or synthesized immediately prior to use ( $\text{ClONO}_2$ ,

HOCl).<sup>42</sup> HOCl was prepared as an equilibrium mixture of  $\text{Cl}_2\text{O}$  and water, while  $\text{ClONO}_2$  was prepared by the reaction of  $\text{Cl}_2\text{O}$  with  $\text{N}_2\text{O}_5$ . All gases were stored at liquid nitrogen temperatures in the dark and were free from contamination. Prior to immediate use, each sample was evaporated into the gas phase and stored in passivated glass reservoirs at room temperature. Gas purity was confirmed using mass spectrometry. Ice films were grown by deposition from a constant pressure of  $5 \times 10^{-7}$  mbar for 30 s at 150 K and either cooled or heated to the appropriate temperature. This method reproducibly generates crystalline ice films of ca. 100 nm thick (deduced from their infrared spectra). Because of the effusive nature of the gas inlet to the chamber, these films are assumed to be of uniform thickness.

## Results

**Reaction between HOCl and HCl.** To study the heterogeneous reaction between HOCl and HCl, experiments were conducted using pure thin films of ice with appropriate adsorbates. Both RAIR and mass spectra were obtained during and after dosing, the latter as thermal desorption profiles. Adsorbed films of HOCl were generated in vacuo by the following method. First, an ice film was deposited at the required temperature upon the thermostated gold foil substrate. This clean ice surface was then exposed to an equilibrium mixture of  $\text{H}_2\text{O}$  and  $\text{Cl}_2\text{O}$  containing HOCl. Earlier studies<sup>42</sup> have established that  $\text{Cl}_2\text{O}$  does not stick to or react directly with the ice surface at temperatures in excess of 140 K; hence this procedure results in the formation of an adsorbed layer of HOCl. The RAIR spectrum of such a film at 145 K is shown in Figure 1. Absorption bands at 2716, 1421, and  $725 \text{ cm}^{-1}$  are present in addition to those of ice and can readily be assigned to the  $\nu\text{OH}$ ,  $\delta\text{OH}$ , and  $\nu\text{OCl}$  modes of HOCl, respectively. These values are shifted from their gas-phase values as expected, given that they are located in a strongly hydrogen bonded aqueous environment. Assignment of the bands has been discussed previously.<sup>42</sup> This film was observed to be stable up to a temperature of ca. 160 K, where the onset of intact HOCl

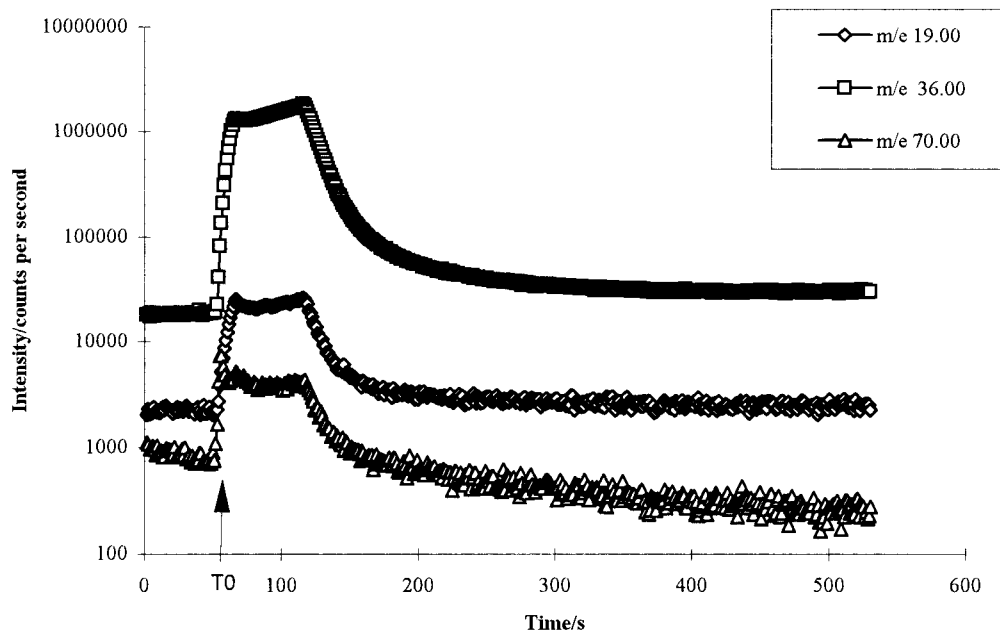


**Figure 3.** Ion traces resulting from the exposure of an HOCl/ice film to gaseous HCl at 145 K. The chlorine signal varies directly with the HCl dose, indicating that it arises from the decomposition of HCl in the mass spectrometer and not from the surface (see text).

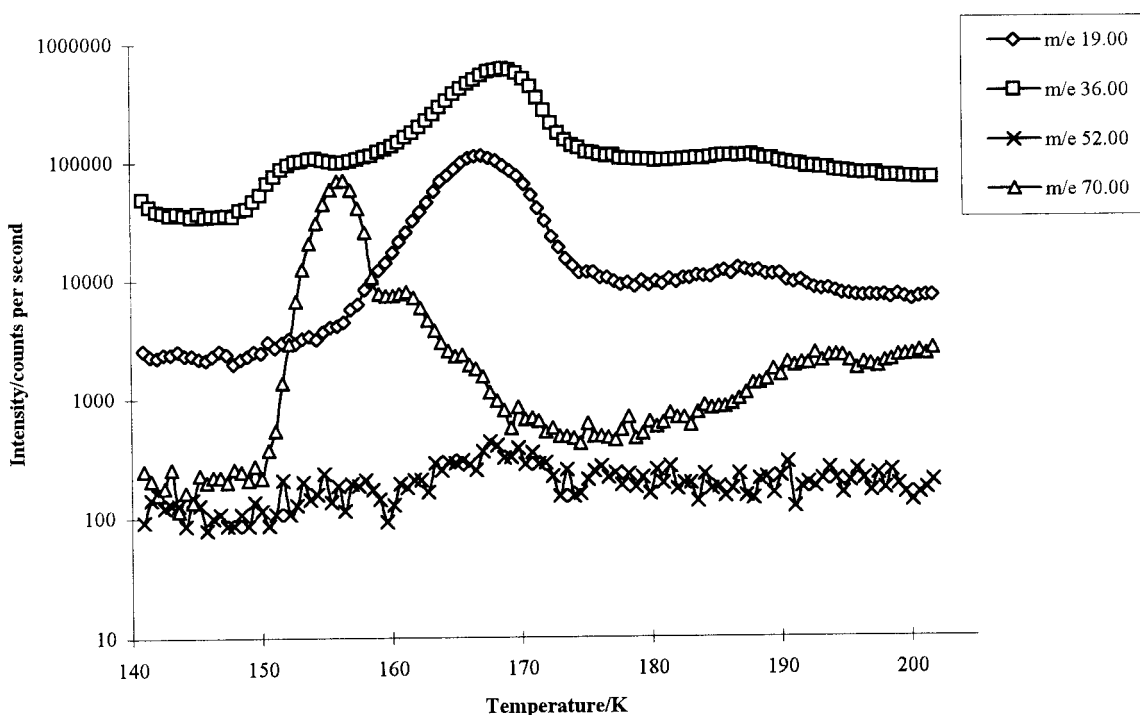


**Figure 4.** Thermal desorption ion traces obtained when heating the HOCl/HCl/ice film from Figure 3 from 140 to 200 K, which clearly shows that the ejection of molecular chlorine above 155 K is not accompanied by any HOCl release.

desorption was observed from the surface. Apart from water, no species other than those expected for the fragmentation of  $^1\text{HO}^{35}\text{Cl}$  ( $m/e$  35, 51, and 52<sup>59</sup>) were observed to accompany the desorption process in the mass spectrum. This behavior concurs with that observed in earlier studies.

Exposure of a film of HOCl adsorbed upon ice to gaseous HCl at 145 K resulted in the growth of infrared absorption features due to the hydrated proton from HCl dissociation and a diminution of the bands due to HOCl in the RAIR spectrum (not shown). The loss of HOCl from the ice surface was quantified by measuring the integrated intensity of the  $\nu\text{OH}$  band of HOCl, shown in Figure 2 as a function of HCl exposure in langmuirs (1 langmuir =  $1 \times 10^{-6}$  Torr s). If, as has previously

been conjectured,<sup>42</sup> this loss of HOCl is due to reaction with  $\text{H}_3\text{O}^+(\text{H}_2\text{O})_n\text{Cl}^-$  to produce  $\text{Cl}_2$ , it should be possible to detect this molecular chlorine by mass spectrometry. This can be achieved either by directly observing the ejection of  $\text{Cl}_2$  in the mass spectrum during dosing or by monitoring its subsequent release in a thermal desorption experiment. Figure 3 shows a multiple ion trace obtained during exposure of the HOCl/ice film to an HCl dose of ca. 15 langmuirs ( $3 \times 10^{-7}$  mbar, 60 s) at 145 K. Dosing was initiated at the time indicated as  $T_0$ . As the signal due to  $^1\text{H}^{35}\text{Cl}^+$  rises ( $m/e$  36), it is followed closely by those due to  $^{35}\text{Cl}_2^+$  ( $m/e$  70) and water (monitored as the overlap of the extremely intense  $\text{H}_2\text{O}^+$   $m/e$  18 signal into the  $m/e$  19 channel of the mass spectrometer to avoid saturation of

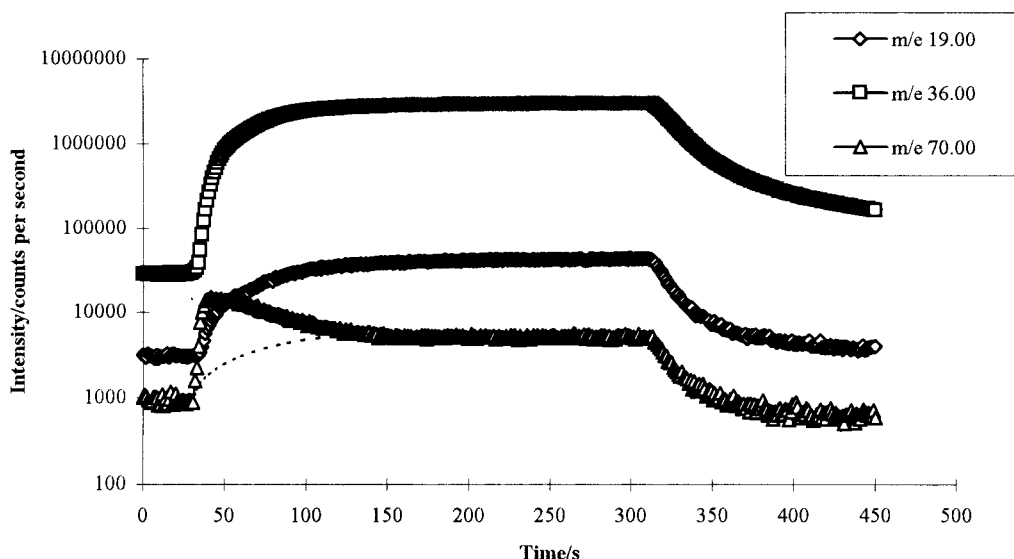


**Figure 5.** Ion traces resulting from the exposure of an HOCl/ice film to gaseous HCl at 155 K. At long exposure times, the chlorine signal shows an underlying trend that varies directly with the HCl dose as in Figure 3, indicated by the dotted line. However, the initial trace shows the ejection of a significant amount of molecular chlorine.

the detector). These signals may arise either by direct ejection of the relevant species from the HOCl/ice surface, because of contamination of the source gases, or by their formation in the ionization region of the mass spectrometer. In the case of water, ejection from the surface is likely to be the dominant process because large water signals are always observed when pure ice films are exposed to HCl, most probably due to the localized heating effect of the enthalpy of solvation of HCl to form ionic hydrates. Similarly, in the absence of any cold substrate in the vacuum system, a small  $^{35}\text{Cl}_2^+$  signal is frequently observed in the mass spectrum of pure HCl (it is usually the main contaminant in lecture-bottle HCl). It therefore seems unlikely that a significant proportion of molecular chlorine is ejected from the surface at this temperature. This assertion is also supported by the fact that, with the exception of a small initial blip in the  $m/e$  70 signal, all three signals show exactly the same intensity trends as a function of time. Under these conditions, then, the reaction products mostly remain on the surface and this experiment can therefore effectively be treated as a blank for the higher temperature mass spectrometric measurements that follow.

If the temperature of the resulting film is raised from 145 K in a thermal desorption experiment, the ejection of  $\text{Cl}_2$  is observed, as shown in Figure 4. The temperature of the desorption maximum of the  $m/e$  70 signal is ca. 155 K and is accompanied by a small increase in the  $^1\text{H}^{35}\text{Cl}^+$  signal. This desorption trace may result from  $\text{Cl}_2$  produced in the lower temperature reaction which remains adsorbed upon the surface. Additionally, since the reaction between dissociated HCl and molecular HOCl requires that the species come into contact, a contribution to this signal may come from the increased rate of surface or bulk diffusion of the reactants toward each other as the temperature increases. It is well-known that both the hydrated protons and chloride ions increase in mobility with temperature,<sup>60,61</sup> and it is therefore possible that some delayed (in temperature) reaction occurs only when ionic diffusion speeds are sufficiently high to enable chloride ions to approach and react with adsorbed HOCl molecules. This assertion is supported by the coincidence between the  $m/e$  70 and 36 signal maxima, since the latter is often observed in the thermal desorption spectra of HCl films through the recombination of mobile  $\text{H}_3\text{O}^+$  and  $\text{Cl}^-$  ions.<sup>47</sup> Figure 4 also demonstrates that,

as the temperature approaches 172 K, film disruption occurs and the entire film evaporates, liberating water and excess HCl. As expected, in the presence of excess adsorbed, ionized HCl there is clearly no trace of HOCl either at low temperature or upon film desorption.

To study the ejection of  $\text{Cl}_2$  directly, an identical film of HOCl adsorbed upon ice was exposed to ca. 60 langmuirs of gaseous HCl ( $3 \times 10^{-7}$  mbar, 280 s) at 155 K. The trend in the ion signals during this exposure is shown in Figure 5. At long exposure times, the underlying trend of the water,  $^1\text{H}^{35}\text{Cl}^+$ , and  $^{35}\text{Cl}_2^+$  traces is the same as at 145 K; that is, each trace responds with the same profile. The main difference occurs in the first few seconds of dosing, where the  $m/e$  70 signal increases rapidly as molecular  $\text{Cl}_2$  is generated and ejected from the film surface. The dotted line in Figure 5 is an estimate of the underlying trend of the signal, the behavior of which at long exposure times appears to indicate saturation. The integrated intensity of the  $\text{Cl}_2$  signal beyond the estimated baseline corresponds within 15% to the integrated intensity of the  $\text{Cl}_2$  desorption peak from the 145 K film. At 155 K, similar to the situation found for the TPD of the lower temperature film, hydroxonium and chloride ion mobility is likely to be sufficiently large to enable the reaction to consume all of the adsorbed HOCl. This is borne out by the RAIR difference spectrum shown in Figure 6, which was obtained from a ratio of the RAIR single beam spectra of an HOCl/ice film before and after exposure to gaseous HCl. This clearly shows loss features due to HOCl and water, consumed as the incoming HCl reacts to produce  $\text{H}_3\text{O}^+(\text{H}_2\text{O})_n$ , for which growth features can be seen. When this film is recooled to 140 K and submitted to a thermal desorption, there is no evidence for either molecular chlorine or HOCl release. Upon film disruption, only HCl and water are observed in significant quantities.

**Reaction between  $\text{ClONO}_2$  and Water.** As described in the Introduction to this paper, previous studies of the heterogeneous hydrolysis of  $\text{ClONO}_2$  at the atmospherically relevant temperature of 180 K have provided strong evidence for the intermediacy of an  $[\text{H}_2\text{OCl}]^+$  ion<sup>43</sup> under conditions of extremely low water availability. In view of the fact that the subsequent hydrolysis of this species to produce gas-phase HOCl in the presence of excess water is rapid at 180 K, the reaction has been studied at lower temperatures, using the mass spectrometer

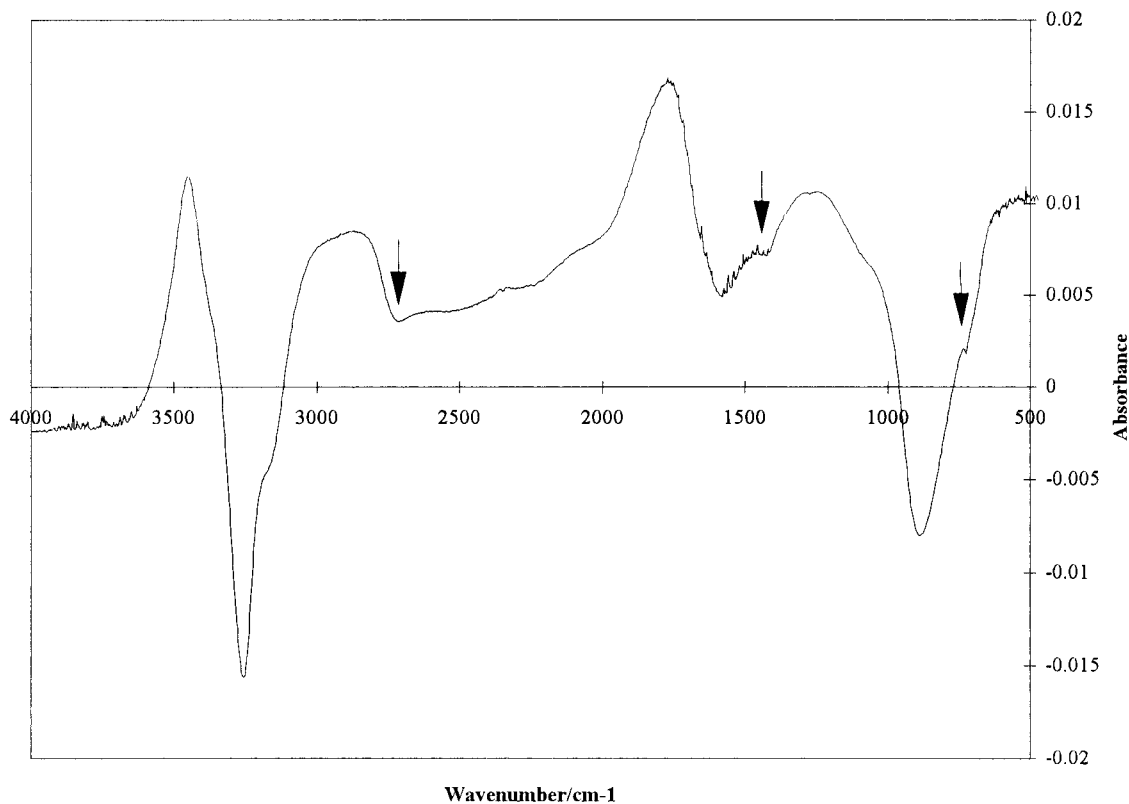


**Figure 6.** RAIR difference spectra obtained from the ratio of spectra before and after exposure to gaseous HCl (corresponding to  $T = 0$  and  $T = 400$  in Figure 5). Features due to HOCl (arrows) and  $H_2O$  loss are evident, along with the growth of bands characteristic of ionized HCl hydrates.

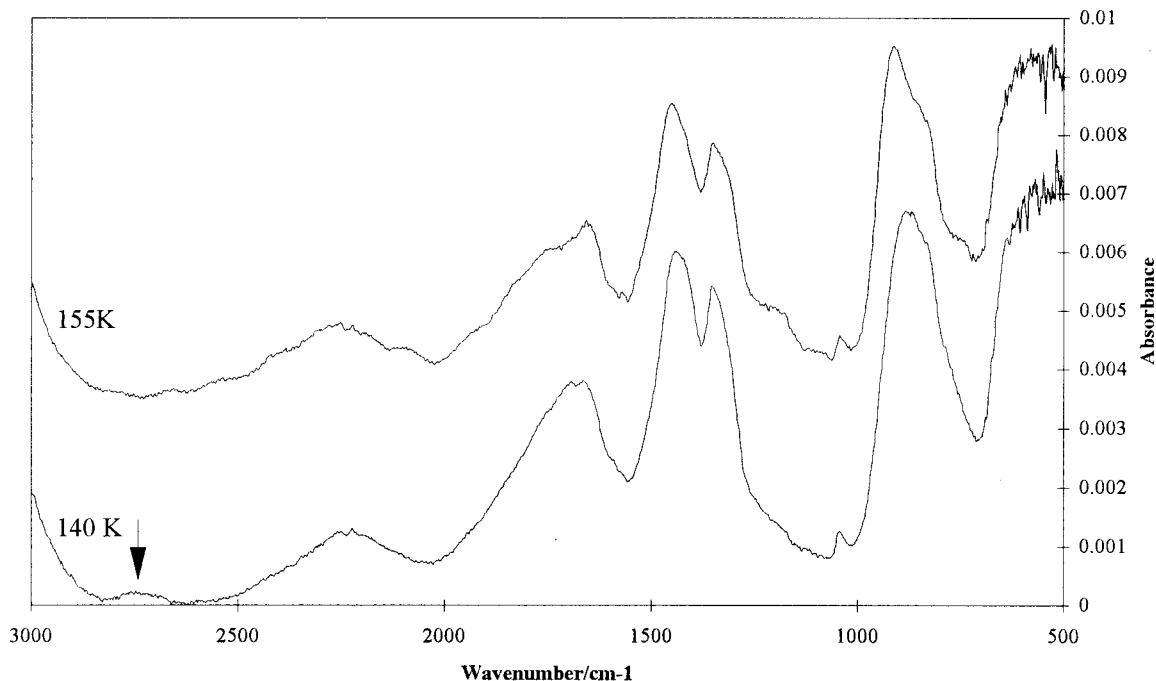


**Figure 7.** RAIR spectra of water and  $ClONO_2$  cocondensed at 140 and 155 K. The most important difference between the two is the presence of the  $\nu_{OH}$  mode of HOCl at  $2722\text{ cm}^{-1}$  in the 140 K spectrum (arrow).

to highlight the retention or loss of specific species from the surface. These experiments are complementary to a series of recent Knudsen cell measurements by Rossi and co-workers.<sup>59</sup> Since the experiments discussed in the previous section suggest that any HOCl produced can be retained in an adsorbed form by an ice film at temperatures below ca. 150 K, reactions were carried out at 140 and 155 K. Cocondensation of water and  $ClONO_2$  at pressures of  $1 \times 10^{-7}$  and  $3 \times 10^{-8}$  mbar, respectively, resulted in the spectra shown in Figure 7. At both

140 and 155 K, these spectra are broadly similar to those observed for exposure of ice to  $N_2O_5$ , with water, hydroxonium, and nitrate ion features at ca.  $3250$ ,  $1750$ , and  $890\text{ cm}^{-1}$ ,  $3000$  and  $1750\text{ cm}^{-1}$ , and  $1450$ ,  $1305$ ,  $1032$ , and  $815\text{ cm}^{-1}$  respectively.<sup>26,31,62,63</sup> These positions are summarized in Table 1. Many of these absorption bands show shifts and broadening due to a wide range of solvation environments within the condensed film, and as expected, the 155 K spectrum shows evidence of being more crystalline through the  $\delta H_3O^+$  and  $\delta H_2O$

**TABLE 1: Infrared Band Positions ( $\text{cm}^{-1}$ ) and Assignments for Nitrate and Chlorine Hydrates, along with Literature Values for Comparison<sup>e</sup>**

Figure 7, 140 K	Figure 7, 155 K	Figure 12, A	Figure 12, D	$\alpha$ -NAT <sup>a</sup>	NAT <sup>b</sup>	HONO <sub>2</sub> <sup>b</sup>	HONO <sub>2</sub> <sup>c</sup>	HCl·6H <sub>2</sub> O <sup>a</sup>	assignment <sup>d</sup>
		3330	3430	3424	3430			3424	} $\nu(\text{H}_2\text{O})$
			3250	3203	3250				
			1880 (sh)			3150			$\nu(\text{OH})$
			1753	1753	1790			1892	$\delta(\text{H}_9\text{O}_4^+)^{67}$
1680 (br)	1750 (br) 1657	1744 (br)							$\delta(\text{H}_3\text{O}^+)$ ( $\nu_4$ ) nitrate and amorphous
			1635 (s)			1690	1682		$\delta(\text{H}_3\text{O}^+)$ ( $\nu_4$ ) nitrate, crystalline
1440	1450	1445						1635	$\delta(\text{H}_3\text{O}^+)$ highly crystalline
1351	1350		1395 (sh)	1393	1390				$\nu_a(\text{NO}_3^-)$ amorphous
			1370						$\nu_a(\text{NO}_3^-)$ NAT ( $\nu_3$ )
						1335	1318		$\nu_a(\text{NO}_3^-)$ NAT ( $\nu_3$ )
									$\nu(\text{NO}_2)$
									$\nu(\text{NO}_3^-)$ amorphous
1042 (w)	1045 (w)	1041 (w)	1117 (br)		1130			1278	$\delta(\text{H}_3\text{O}^+)$ ( $\nu_2$ )
880 (br)	914		1030 (br, w)	1110					$\nu_s(\text{NO}_3^-)$ NAT ( $\nu_1$ )
									$\delta(\text{H}_2\text{O})$
									$\delta(\text{HONO}_2)$
83- (sh)	830 (sh)	820 (w)	820 (s)	820	820			965	$\delta_{\text{op}}(\text{NO}_3^-)$ ( $\nu_2$ )
		782 (w)	782	776					$\delta(\text{H}_3\text{O}^+)$ (torsion)
									$\delta(\text{NO}_2)$
						772	778		

<sup>a</sup> Ritzhaupt and Devlin, ref 67. <sup>b</sup> Koch et al., ref 91. <sup>c</sup> Horn et al., ref 62. <sup>d</sup> Ritzhaupt and Devlin<sup>67</sup> mode labels in parentheses. <sup>e</sup> Symbols: sh, shoulder; br, broad; w, weak; s, strong.

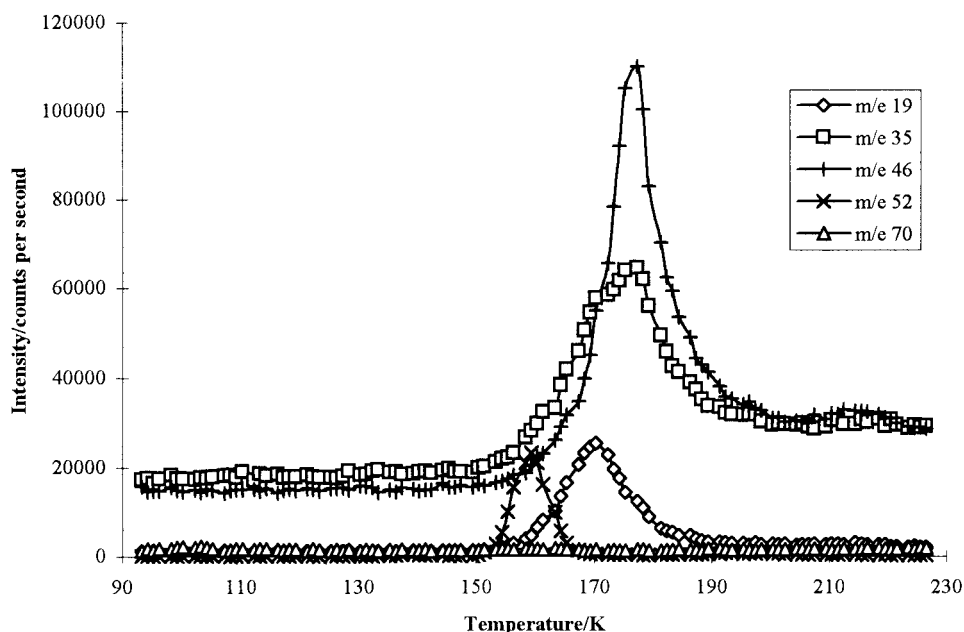


**Figure 8.** Thermal desorption ion traces observed when a 140 K ClONO<sub>2</sub>/ice film (corresponding to the 140 K trace in Figure 7) is heated from 90 to 220 K. The HOCl desorption trace at  $m/e$  52 is not correlated to the  $m/e$  46 peak of NO<sub>2</sub><sup>+</sup>.

features in the 1800–1600  $\text{cm}^{-1}$  region. No strong features attributable to molecular nitric acid are evident, which would give rise to absorption bands at 1683, 1315, 965, and 778  $\text{cm}^{-1}$ .<sup>26,62,64,65</sup> Similarly, there are no obvious strong absorption features at 1734, 1300, 821, 786, and 710  $\text{cm}^{-1}$ , which would indicate the presence of significant amounts of adsorbed molecular chlorine nitrate,<sup>66</sup> although the mass spectrometric evidence suggests that there may be a trace of unreacted material trapped in the ice matrix (discussed below). When compared to higher temperature cocondensation spectra, which show similar nitrate ion features, the feature previously attributed to H<sub>2</sub>OCl<sup>+</sup> at 1650  $\text{cm}^{-1}$ <sup>66</sup> also appears to be insignificant in the 140 K spectrum. A significant amount of this species would suggest that insufficient amounts of water were available during film deposition, which is unlikely to be the case. A further important difference is the presence of a weak but distinct

feature at 2722  $\text{cm}^{-1}$  in the 140 K spectrum, which, by reference to the preceding spectra, is attributable to the presence of molecular HOCl.

This assignment is supported by the thermal desorption profiles of such a film, shown in Figure 8, obtained by first cooling the film to 90 K. This clearly shows the onset of the desorption of a species with  $m/e$  52 (<sup>1</sup>HO<sup>35</sup>Cl) from ca. 150 K. Other species monitored in this thermal desorption experiment include <sup>35</sup>Cl<sup>+</sup> ( $m/e$  35), NO<sub>2</sub><sup>+</sup> ( $m/e$  46), and water ( $m/e$  19). As the mixed film disrupts, these traces show the simultaneous desorption of water and a chlorine-containing species above ca. 170 K. Thermal desorption from the 155 K film shows a rather different set of desorption profiles (Figure 9). In comparison to the 140 K desorption profiles, there is an insignificant increase in the  $m/e$  52 signal at 155 K. At 170 K, the traces show the same desorption of <sup>35</sup>Cl<sup>+</sup>, NO<sub>2</sub><sup>+</sup>, and water as before. However,

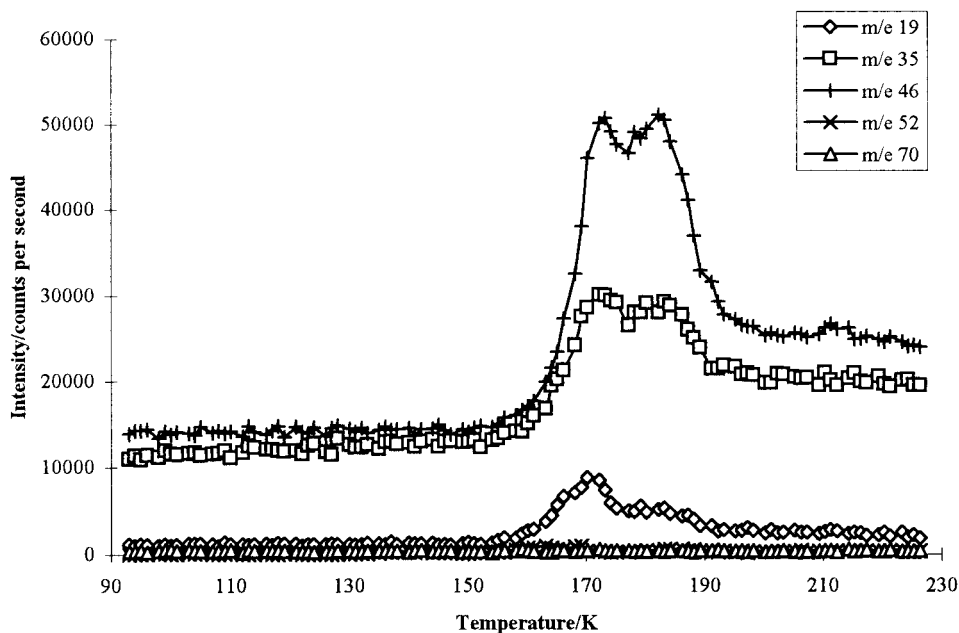


**Figure 9.** Thermal desorption ion traces observed when a 155 K ClONO<sub>2</sub>/ice film (corresponding to the 155 K trace in Figure 7) is heated from 90 to 220 K. In this case, no HOCl evolution is observed.

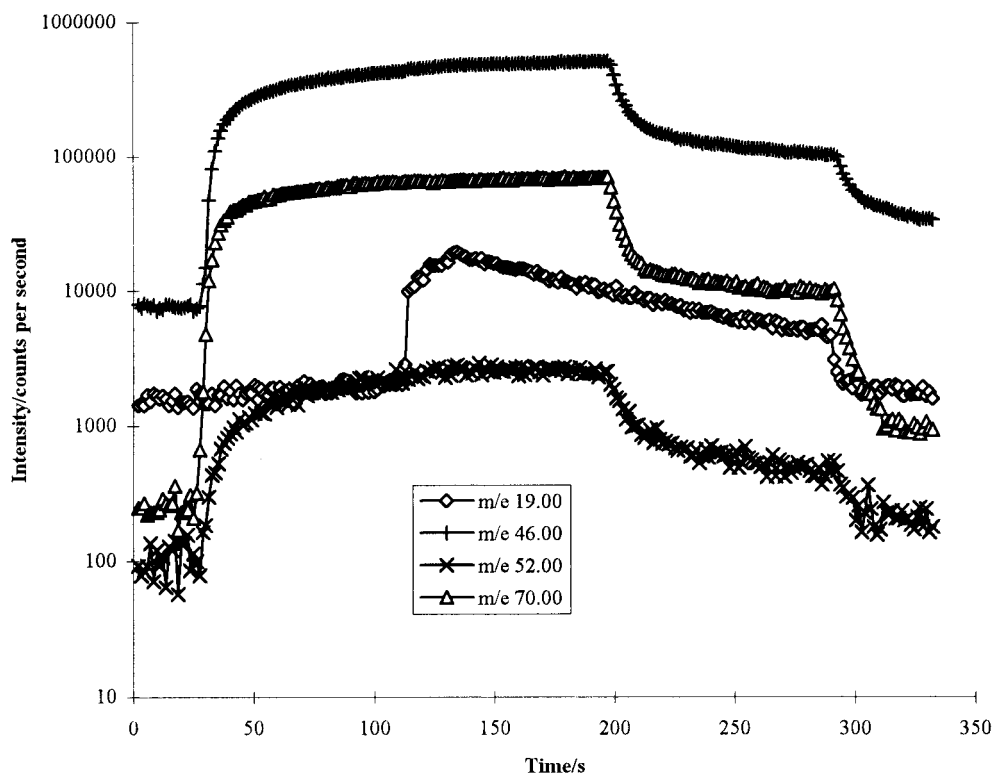


**Figure 10.** Ion traces obtained during cocondensation of ClONO<sub>2</sub> and water at 140 K. The use of a logarithmic scale shows that the weak *m/e* 52 trace is clearly correlated to the *m/e* 46 trace characteristic of the fragmentation of ClONO<sub>2</sub>. There is clearly no correlation with variations in the *m/e* 19 trace used to monitor water, indicating that HOCl is not being ejected into the gas phase from the surface.

a secondary desorption at higher temperature is also observed, which we ascribe to a crystallinity effect in the residual nitric acid hydrate film, similar to that observed for the  $\alpha$ - to  $\beta$ -NAT transformation.

Further corroboration of this HOCl retention or ejection phenomenon is obtained by monitoring the mass signals due to water, NO<sub>2</sub><sup>+</sup>, <sup>1</sup>HO<sup>35</sup>Cl<sup>+</sup>, and <sup>35</sup>Cl<sub>2</sub><sup>+</sup> during simultaneous water and ClONO<sub>2</sub> dosing at different temperatures, shown in Figures 10 and 11. At 140 K (Figure 10), the signals due to NO<sub>2</sub><sup>+</sup>, <sup>1</sup>HO<sup>35</sup>Cl<sup>+</sup>, and <sup>35</sup>Cl<sub>2</sub><sup>+</sup> follow the same profile over the entire

dose. Increasing the water pressure at ca. 110 s does not affect the HOCl signal, indicating that no additional HOCl is released into the gas phase. However, this is not the case at 155 K, where the <sup>1</sup>HO<sup>35</sup>Cl<sup>+</sup> signal clearly shows a component that tracks the water profile exactly. This result explains the absence of HOCl in the 155 K thermal desorption, since any HOCl formed is directly released into the gas phase.

**Reaction between ClONO<sub>2</sub> and H<sub>3</sub>O<sup>+</sup>(H<sub>2</sub>O)<sub>*n*</sub>Cl<sup>-</sup>.** The reaction between gaseous ClONO<sub>2</sub> and HCl was studied using a film with an appreciable concentration of hydrated ionic HCl



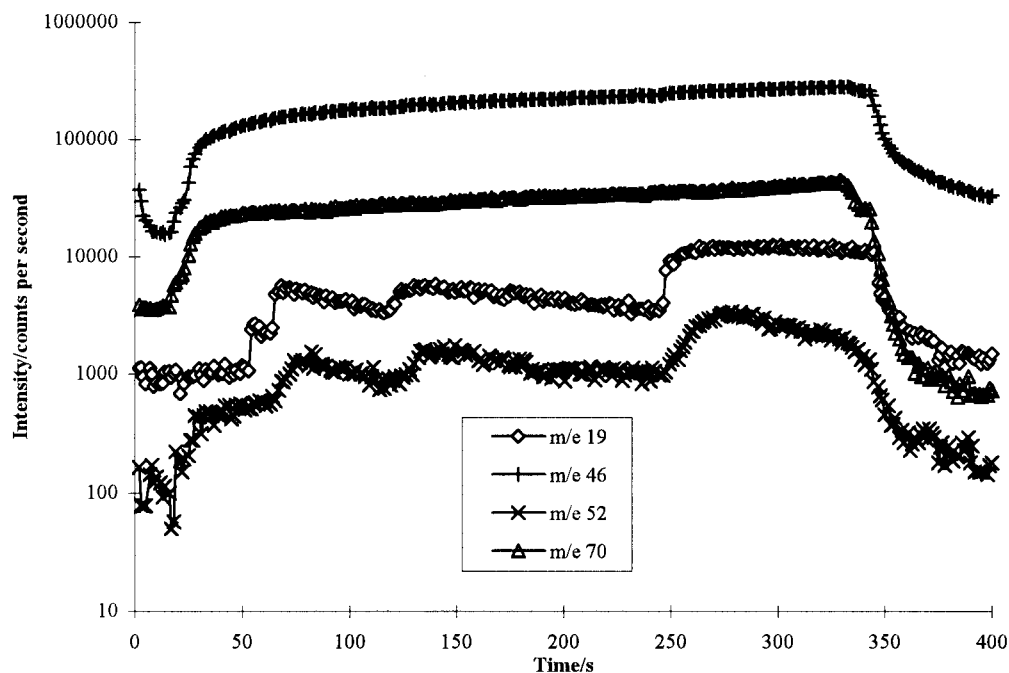


**Figure 11.** Ion traces obtained during cocondensation of  $\text{ClONO}_2$  and water at 155 K. In this case, the  $m/e$  52 HOCl trace is clearly correlated with both the  $m/e$  46 trace characteristic of the fragmentation of  $\text{ClONO}_2$  and variations in the  $m/e$  19 trace used to monitor water, indicating that HOCl is being ejected into the gas phase from the surface.

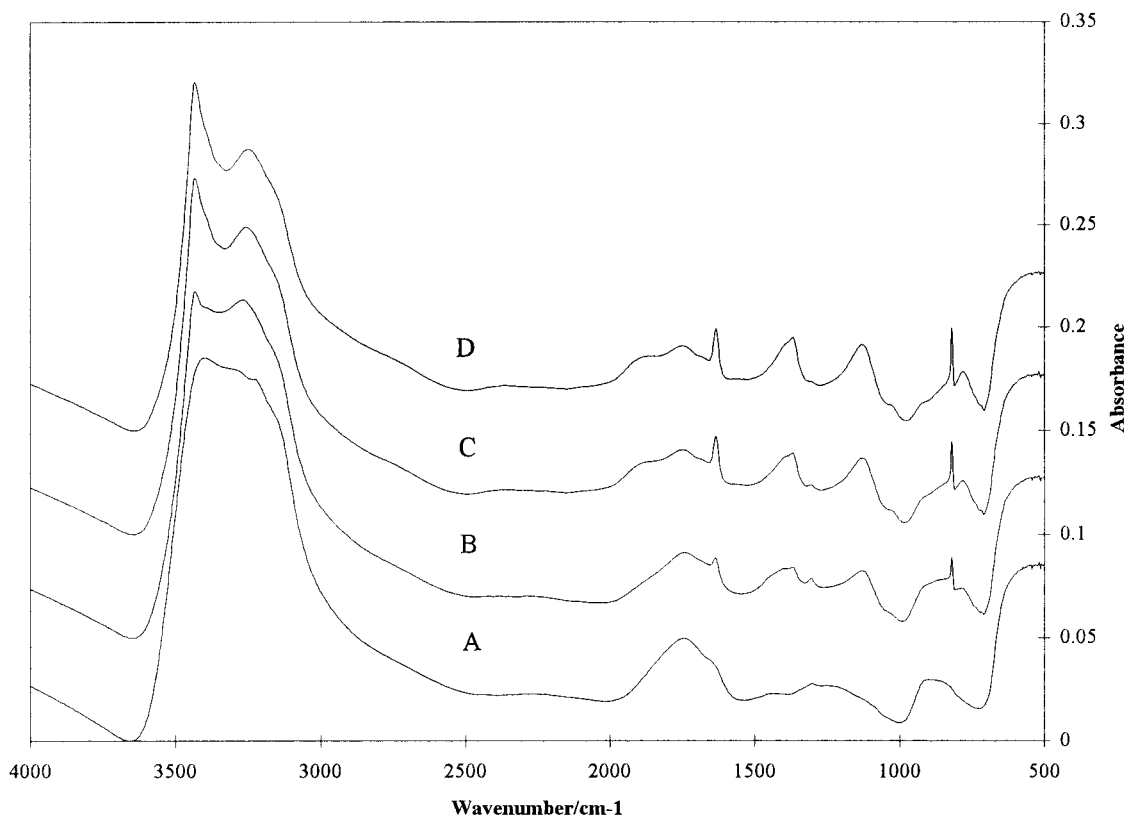


**Figure 12.** RAIR spectra resulting from the exposure of an ionic HCl hydrate film to gaseous  $\text{ClONO}_2$  at a constant pressure of  $5 \times 10^{-5}$  mbar at 160 K: (A) pure  $\text{H}_3\text{O}^+(\text{H}_2\text{O})_n\text{Cl}^-$ ; (B) 25 s  $\text{ClONO}_2$ ; (C) additional 25 s  $\text{ClONO}_2$ ; (D) saturation ( $>100$  s total  $\text{ClONO}_2$ ).

as a substrate. This film was formed by cocondensing HCl and water at partial pressures of  $2 \times 10^{-7}$  and  $8 \times 10^{-7}$  mbar, respectively, upon the gold substrate at 160 K for 250 s. The RAIR spectrum of the resulting film, shown in Figure 12, trace A, exhibits features that are readily assigned to a semiamorphous film of HCl hydrate of indeterminate stoichiometry. Band assignments for such a film have been discussed extensively in the literature.<sup>51,67</sup> Of particular note, however, is the intense

$3300 \text{ cm}^{-1}$  band due to the  $\nu\text{OH}$  modes of both  $\text{H}_2\text{O}$  and  $\text{H}_3\text{O}^+(\text{H}_2\text{O})_n$ . At 160 K, this film is partially crystalline; this is reflected in the spectrum, which shows structure in the  $\nu\text{OH}$  and  $\delta\text{OH}$  bands and the onset of spectral perturbations introduced by optical effects of the reflection geometry used to record spectra.<sup>68</sup>

The result of exposing this film to gaseous  $\text{ClONO}_2$  at a partial pressure of  $5 \times 10^{-7}$  mbar was monitored using both

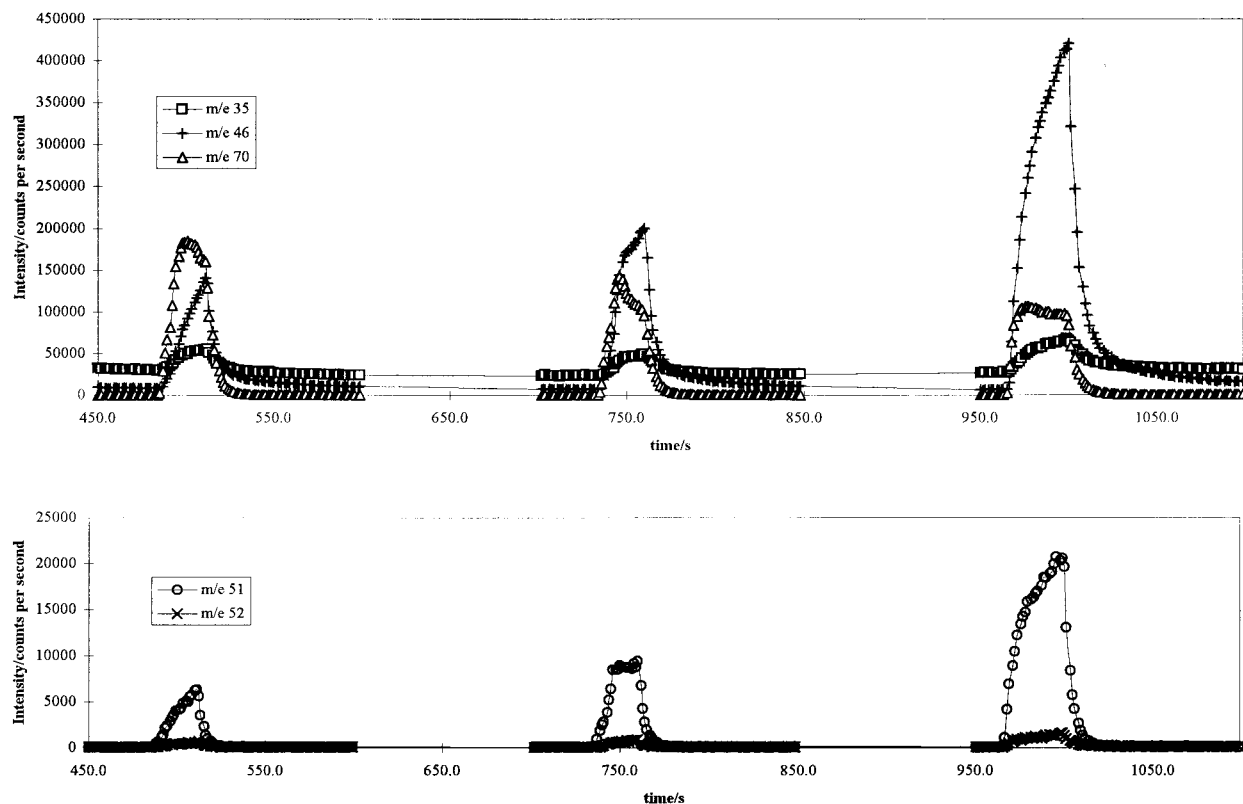


**Figure 13.** Ion traces obtained during the exposures described in Figure 12 for the key species  $\text{H}_2\text{O}^+$ ,  $\text{HCl}^+$ ,  $\text{NO}_2^+$ ,  $\text{ClO}^+$ ,  $\text{HOCl}^+$ , and  $\text{Cl}_2^+$ .

RAIRS and mass spectrometry. Traces B and C in Figure 12 show the RAIR spectra obtained following  $\text{ClONO}_2$  exposures of 40 and 60 s, while trace D shows the result of exposing the film to  $\text{ClONO}_2$  until no further spectral change occurred (i.e., saturation). The most obvious changes resulting from increased exposure are the growth of strong features at 3432, 3249, 1634, 1369, 1131, and 820  $\text{cm}^{-1}$ . There are also clear changes in the prominent features at ca. 1750 and 900  $\text{cm}^{-1}$  assigned to water and the hydrated  $\text{H}_3\text{O}^+$  ion. The majority of the features that grow in with exposure are readily assigned to crystalline forms of NAT and HCl hydrates by reference to published spectra.<sup>33,63,67</sup> A sharp band is also present at 1635  $\text{cm}^{-1}$ , which may be assigned to absorption from a well-ordered proton in an ion such as  $\text{H}_5\text{O}_2^+$  or  $\text{H}_7\text{O}_3^+$ .<sup>67</sup> Band positions and assignments are also summarized in Table 1. Closer examination of the 2700  $\text{cm}^{-1}$  region (via absorption-difference spectra, not shown) also indicates that there is no trace of the feature noted earlier due to molecular adsorbed HOCl at 2722  $\text{cm}^{-1}$ . These spectra indicate therefore that the heterogeneous reaction of gas-phase  $\text{ClONO}_2$  with condensed, hydrated HCl films results in the formation of condensed nitric acid hydrates as expected.

Mass spectrometric monitoring of the gases present above the substrate surface during each  $\text{ClONO}_2$  exposure is shown in Figure 13. In each case, a specific amount (pressure  $\times$  time) of  $\text{ClONO}_2$  was deposited onto the substrate surface. For the first dose, a rapid rise in the  $m/e$  70 signal due to  $^{35}\text{Cl}_2^+$  is observed. This observation is accompanied by a more gradual rise in the  $^{35}\text{Cl}^+$ ,  $\text{NO}_2^+$ , and  $^{35}\text{ClO}^+$  signals due to the direct ionization of the admitted  $\text{ClONO}_2$ , which once again is confirmed by their identical profiles. Subsequent doses show similar behavior for these fragmentation components. However, the  $^{35}\text{Cl}_2^+$  signal rapidly decreases with cumulative exposure. In dose 2, which corresponds to the RAIR spectrum in Figure 12, trace B, the  $m/e$  70 signal again rises rapidly (although to

a much lower level), but then falls with increasing dose time. Concomitantly, the other signals due to the  $\text{ClONO}_2$  dose rise. It can also be seen that the  $\text{ClONO}_2$  fragmentation signals achieve a much higher value than in dose 1, although the actual pressure of gas admitted to the chamber is the same in all doses. This behavior is much more marked in the third exposure, which shows a significantly reduced  $m/e$  70 signal compared to the  $\text{ClONO}_2$  fragmentation signals. A clarification of this trend is obtained by simply plotting the  $m/e$  70 signals for each exposure next to each other. If the underlying linear component is neglected (since it is due to the fragmentation and recombination of  $\text{ClONO}_2$ : see earlier), this trend is strongly reminiscent of a saturation curve.

## Discussion

**Reaction between HOCl and HCl.** The HOCl/HCl/ $\text{H}_2\text{O}$  system measured here sheds further light onto the mechanisms whereby reactions occur in heterogeneous atmospheric systems based upon water ice. It is clear from both earlier studies<sup>42</sup> and the infrared and mass spectrometric evidence presented here that molecular HOCl adsorbed upon the surface of water ice at low temperature is converted to  $\text{Cl}_2$  by reaction with  $\text{H}_3\text{O}^+\text{Cl}^-$ . It seems also apparent that the initial fate of the reaction product (i.e., release or continued adsorption) depends solely upon the substrate temperature. It is also clear, since even the partial conversion of HOCl to  $\text{Cl}_2$  at temperatures as low as 140 K is accompanied by the formation of hydroxonium ion bands during the reaction, that the reaction requires the HCl to be in a hydrated ionic form; that is, the reaction is between HOCl and  $\text{Cl}^-$ . Similarly, the lack of evidence of HOCl desorption in the thermal desorption traces from either the 145 or 155 K film in the presence of excess HCl indicates that the reaction is very efficient, even at these low temperatures. The fact that HOCl itself does not appear to form an ionic hydrate on water ice surfaces (as we have observed previously<sup>43</sup>) is entirely consistent

with the fact that HOCl is much less acidic than HCl and, if anything, is much more likely to be dechlorinated than deprotonated. Theoretical studies support this picture of HOCl molecular adsorption, with weak surface HOCl attachment occurring via a number of hydrogen bonds at low temperatures.<sup>69,70</sup> Direct HOCl desorption from the ice surface at temperatures in the range 150–160 K<sup>42</sup> also indicates that it is not strongly bound to solid ice (although the case may be very different for liquid water or sulfuric acid solutions,<sup>71</sup> where the bulk solubility may be appreciable and *absorption* may occur) and is therefore unlikely to be present for significant periods of time at stratospheric temperatures. Drawing this evidence together, it appears that the ice-catalyzed heterogeneous reaction between HOCl and HCl at stratospheric temperatures depends on the presence of adsorbed Cl<sup>-</sup> ions. The reaction then occurs when impinging HOCl molecules appear transiently at the surface, reacting with Cl<sup>-</sup> ions in a manner reminiscent of the Eley-Rideal mechanism of surface reaction kinetics.<sup>72</sup> (N.B. The Eley-Rideal reaction scheme technically only describes the kinetics of monolayer surface reactions and is not directly applicable to reactions on ice because the materials involved are not necessarily confined to a pure surface monolayer.)

**Reaction between ClONO<sub>2</sub> and Water.** In agreement with numerous other studies, the reaction of chlorine nitrate with water ice at low temperatures clearly leads to the formation of HOCl, evidenced by its characteristic signature in the IR and mass spectra presented here. The infrared spectra resulting from an exposure of ice to ClONO<sub>2</sub> clearly show the presence of hydrated H<sub>3</sub>O<sup>+</sup> and NO<sub>3</sub><sup>-</sup> ions at both temperatures. There are some subtle features due to crystallinity evident in the higher temperature spectra, which tally with the observations of other studies. When nitric acid hydrates are at least partially crystalline, the 1800–1600 cm<sup>-1</sup> region becomes rather complicated. As discussed extensively by Ritzhaupt and Devlin,<sup>67</sup> the species present may include an amorphous component along with the mono-, di-, and trihydrate of the nitrate ion. Some of these species have reasonably characteristic proton hydrate deformation modes, but in general they are not sufficiently well resolved for accurate assignment. However, it is clear that there are no significant amounts of molecular HONO<sub>2</sub> present under these conditions, since the majority of the absorption bands attributable to this species are absent. This is a significant point of dispute among workers in this area. Bianco and Hynes<sup>74</sup> have recently advocated an alternative assignment of the vibrational features present in spectra obtained in an earlier study of ClONO<sub>2</sub> reaction and hydrolysis by Sodeau et al.,<sup>66</sup> in which the formation of an [H<sub>2</sub>OCl<sup>+</sup>] ion is suggested at high temperatures (180 K) and low water availability, suggesting that a strong feature at ca. 1650 cm<sup>-1</sup> be assigned to the OH deformation of molecular HONO<sub>2</sub>. However, this assignment is not supported by the spectra presented by Sodeau et al. for the reasons stated above: for molecular HONO<sub>2</sub> to be present, a number of its other absorption features would be identifiable (with appropriate relative intensities<sup>62,91</sup>). Furthermore, we have recently reinvestigated the low-temperature (<140 K) hydrolysis of ClONO<sub>2</sub> under conditions of reduced water availability and have observed the features of molecular HONO<sub>2</sub> directly.<sup>92</sup> In this low-temperature study in the presence of excess water, the absence of spectral features attributable to the [H<sub>2</sub>OCl<sup>+</sup>] ion is as expected, since this species undergoes rapid hydrolysis to produce HOCl (N.B., a time delay before its ejection, such as that observed by Rossi et al.,<sup>59</sup> would not be observed upon the time scale of these measurements). For this reason, we assign the weak 1657 cm<sup>-1</sup> feature in Figure 7 (Table 1) to the effect

of crystallinity in the proton hydrate rather than [H<sub>2</sub>OCl<sup>+</sup>] or molecular HONO<sub>2</sub>.

In a manner similar to the Cl<sub>2</sub> generated by the reaction of HOCl with ionized HCl described above, the immediate fate of the other reaction product, HOCl, depends solely upon substrate temperature: the HOCl formed from the hydrolysis reaction appears to be either retained on the surface (or in the bulk) of the film or released into the gas phase. The critical temperature regime once again appears to be around the 150–160 K desorption temperature of HOCl. As before, this suggests that any HOCl generated by the heterogeneous hydrolysis of ClONO<sub>2</sub> is unlikely to stay bound to an ice surface at stratospheric temperatures. Since the diffusion of HOCl into the ice bulk at low temperatures is also likely to be small (comparable to that of H<sub>3</sub>O<sup>+</sup>Cl<sup>-</sup> ≈ 10<sup>-15</sup> m<sup>2</sup> s<sup>-1</sup> @ 155 K<sup>73</sup>), the bulk of any ice crystal is unlikely to support a significant concentration of HOCl either. This is borne out by the thermal desorption profiles shown in Figures 8 and 9, which clearly show that all the HOCl formed desorbs before ca. 155 K (either directly or subsequently, depending upon experimental conditions) and that no further HOCl is released when the film disrupts. The origin of the chlorine-containing species in the mass spectra upon total film disruption could be due to one of several sources. The first possibility arises because of the method of deposition, which entails cocondensing ClONO<sub>2</sub> and H<sub>2</sub>O. This gives rise not only to HOCl and nitric acid hydrate products but also to unreacted, trapped ClONO<sub>2</sub>. As the water matrix breaks up, this material will be released (it is well above its normal desorption temperature), giving rise to the *m/e* 35 feature. A second, more likely possibility is that the *m/e* 35 signal arises because of the effect of the large water partial pressure that occurs upon film disruption (N.B. the peak monitored is *m/e* 19, which is an overlapping channel to the true *m/e* 18 <sup>1</sup>H<sub>2</sub><sup>16</sup>O signal; the true water partial pressure in the chamber during disruption is *very* large). This water pulse may produce chlorine-containing species by reaction with residual contaminants in the vacuum chamber, particularly in the ionization region of the mass spectrometer.

**Reaction between ClONO<sub>2</sub> and H<sub>3</sub>O<sup>+</sup>(H<sub>2</sub>O)<sub>*n*</sub>Cl<sup>-</sup>.** In the reaction between gaseous ClONO<sub>2</sub> and the HCl-doped ice film, a variety of interesting features are observed in the infrared spectra. First, an amorphous nitric acid hydrate forms (Figure 12, trace A) because of the plentiful availability of surface water. As exposure continues, two distinct sets of features are observed in addition to the underlying ice and amorphous HCl hydrate features. First, the characteristic absorption bands of a highly ordered proton hydrate are seen at 3430, 1880, 1307, and 782 cm<sup>-1</sup>. By comparison to the work of Ritzhaupt and Devlin, these features are assigned to the hexahydrate of HCl. This transformation from amorphous HCl hydrate to a crystalline hexahydrate is due to the consumption of a proportion of the Cl<sup>-</sup> ions close to the surface with a concomitant reduction in the Cl<sup>-</sup>/H<sub>2</sub>O ratio. Accompanying the growth of these features are absorption bands due to α-NAT at 3424, 3250, 1753, 1395, 1131, and 820 cm<sup>-1</sup> (note that the absorption wavenumbers observed here are closer to those observed in other experiments using the RAIRS configurations because of band shifts and distortions caused by the underlying metal and ice substrates). Once again, there is no evidence for the formation of molecular nitric acid, even though the conditions produce a very low surface water availability.

The mass spectrometric measurements accompanying the infrared spectra confirm the generation of Cl<sub>2</sub>. It can be clearly seen from Figures 13 and 14 that a large amount of chlorine is

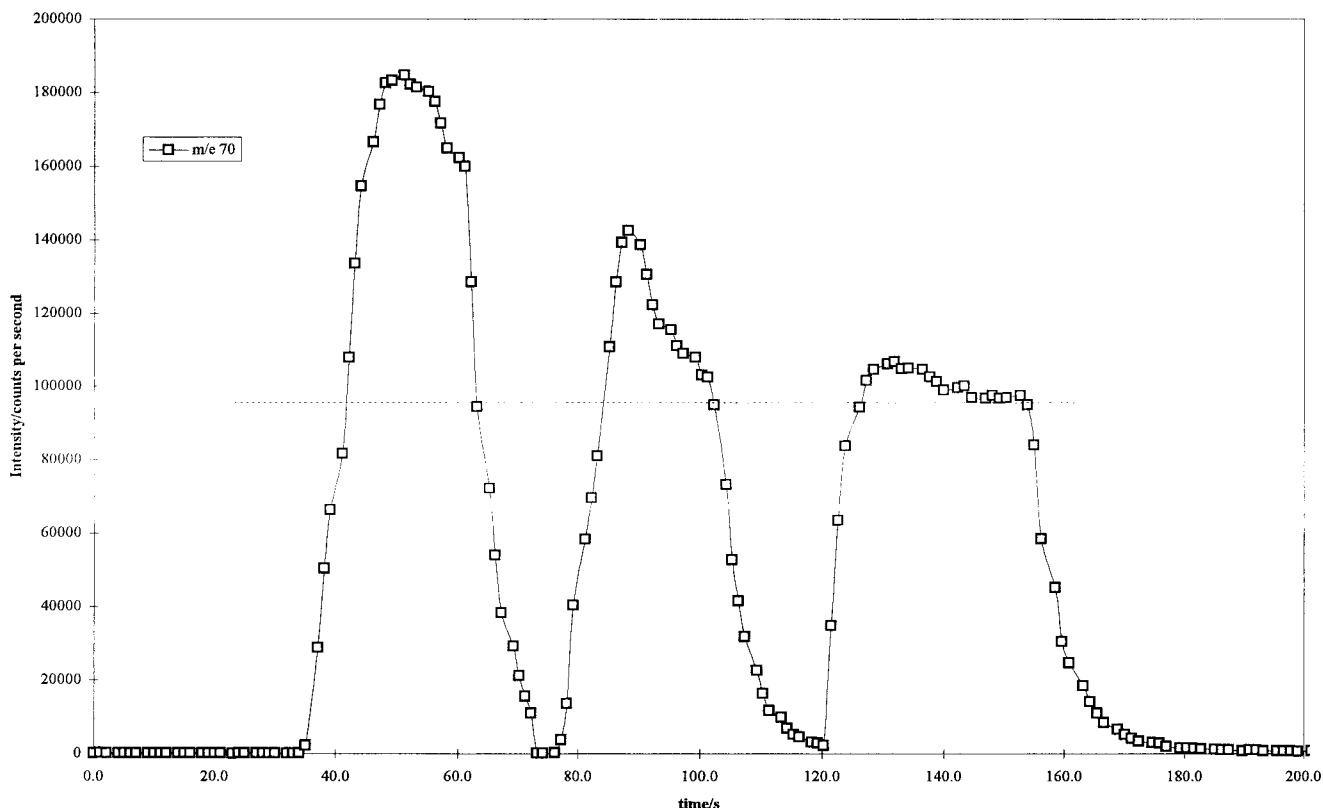


**Figure 14.** Expanded  $m/e$  70 trace of molecular  $\text{Cl}_2$  from Figure 13. The traces have been artificially offset in time for clarity. The dashed line indicates the baseline level, which is due to the residual signal from  $\text{Cl}_2$  generated in the mass spectrometer from  $\text{ClONO}_2$ .

generated and released from the surface. Furthermore, the production of chlorine is instantaneous upon  $\text{ClONO}_2$  exposure and saturates as the amount of surface  $\text{Cl}^-$  is used up. This is corroborated by the behavior of the  $m/e$  46 signal characteristic of  $\text{ClONO}_2$ , which shows that increasingly large amounts of material are directly scattered from the surface without reaction as the depletion of surface  $\text{Cl}^-$  increases. These observations support a direct reaction between incoming, gaseous  $\text{ClONO}_2$  and surface chloride. The absence of any  $\text{HOCl}$  in the mass spectra indicates that the indirect hydrolysis route does not appear to be favored. This is unsurprising, given the greater effectiveness of  $\text{Cl}^-$  as a nucleophile compared to  $\text{H}_2\text{O}$ .

**Reaction Mechanisms.** These observations support the conjecture that the direct reaction of *preadsorbed*  $\text{HOCl}$  (resulting either from direct adsorption or from the  $\text{ClONO}_2$  hydrolysis reaction) with any other surface species is unlikely to play a significant role in the atmospheric chemistry of pure water ice particles at temperatures prevailing in the stratosphere because any  $\text{HOCl}$  formed from  $\text{ClONO}_2$  hydrolysis will be released promptly back into the gas phase. The heterogeneous reactions of  $\text{HOCl}$  are therefore most likely to occur when gas-phase  $\text{HOCl}$  impinges upon an appropriate reaction surface.

The reaction mechanism of  $\text{ClONO}_2$  with a water ice surface appears to be controlled by the relative nucleophile/electrophile strengths of the species involved. However, as a result of an *ab initio* modeling study, it has been recently suggested by Hynes et al.<sup>74</sup> that water itself is too weak an electrophile to attack  $\text{ClONO}_2$  directly. If this is the case, then chlorine nitrate hydrolysis, like the direct hydrolysis of  $\text{HOCl}$  or its reaction with molecular  $\text{HCl}$ , should be unfavorable. The solution to this paradox comes from an examination of earlier spectroscopic studies of both  $\text{N}_2\text{O}_5$  and  $\text{ClONO}_2$  hydrolysis upon ice. When  $\text{N}_2\text{O}_5$  is adsorbed as a thin solid film on any cold substrate, it forms as a covalent molecular layer at low temperatures and as

nitronium nitrate,  $\text{NO}_2^+\text{NO}_3^-$ , at temperatures in excess of 120 K. RAIR and temperature-programmed infrared spectra of ice/ $\text{N}_2\text{O}_5$  layers and cocondensed mixtures indicate that when condensed in either its molecular form or its fully ionized form,  $\text{N}_2\text{O}_5$  does not react directly with water ice.<sup>62,75</sup> This experimental evidence appears to suggest that, in order for reaction to occur,  $\text{N}_2\text{O}_5$  and water have to approach each other at exactly the moment that ionization starts to occur. We have suggested previously that this reaction proceeds at large water excess via a protonated nitric acid intermediate (essentially a complex between  $\text{NO}_2^+$  and  $\text{H}_2\text{O}$ ) to produce two  $\text{H}_3\text{O}^+$  and two  $\text{NO}_3^-$  ions.<sup>43</sup> It seems reasonable to conclude therefore that it is the *process* of ionization which contributes to the reactivity of  $\text{N}_2\text{O}_5$  with water.

When deposited as a thin film at temperatures approaching 180 K,  $\text{ClONO}_2$  has been observed to spontaneously ionize to produce  $\text{Cl}^+\text{NO}_3^-$ .<sup>66</sup> The paradoxical  $\text{H}_2\text{O}/\text{ClONO}_2$  reactivity is then resolved if the reaction that is observed is actually between water and  $\text{Cl}^+\text{NO}_3^{\delta-}$ , i.e. with  $\text{ClONO}_2$  in the process of ionizing, producing  $[\text{H}_2\text{OCl}^+]$  and  $\text{NO}_3^-$  ions as previously described when only a small amount of water is available. The increased reactivity toward ice observed in this system is then due to the increased electrophilicity of the slightly positively charged chlorine atom rather than the nucleophilicity of water. This incidentally also helps to explain the reactivity of  $\text{ClONO}_2$  toward organic liquids as observed by Hanson,<sup>76</sup> wherein an alternative, more reactive form of  $\text{ClONO}_2$  can be formed in the absence of water. The tendency of  $\text{ClONO}_2$  to dissociate along the  $\text{Cl}-\text{O}$  bond is supported by numerous experimental and theoretical studies of the bond strengths and polarizabilities of  $\text{ClONO}_2$ ,<sup>77-79</sup> which suggest that the  $\text{Cl}-\text{O}$  bond is long, weak, and easily polarized positively at the chlorine end.

A far more likely scenario in the atmospheric chemistry of a  $\text{ClONO}_2$  molecule than that of direct hydrolysis is that it will

impinge upon a particle which is coated with chloride ions. In the final series of experiments presented here, further corroboration of a partially ionization precursor mechanism is obtained from the high reactivity between gaseous  $\text{ClONO}_2$  and adsorbed  $\text{Cl}^-$ . Flow tube studies of chlorine nitrate hydrolysis by ice indicate that a certain time delay occurs before the release of HOCl from the surface. If, as has been suggested by Rossi and co-workers,<sup>59</sup> this delay is due to the formation and subsequent hydrolysis of the  $[\text{H}_2\text{OCl}^+]$  ion, then a delay should *not* be observed when  $\text{ClONO}_2$  reacts with  $\text{Cl}^-$  ions because the desorbing species  $\text{Cl}_2$  is formed directly from the reaction.  $\text{H}_3\text{O}^+$  is already present upon the surface as the partner ion of  $\text{Cl}^-$ , and reaction occurs between the partially ionized  $\text{ClONO}_2$  and  $\text{Cl}^-$  to yield gaseous  $\text{Cl}_2$  and adsorbed  $\text{NO}_3^-$ . The direct reaction of  $\text{ClONO}_2$  with adsorbed  $\text{Cl}^-$  ions has also been recently observed in SIMS measurements by Donsig et al.<sup>80–82</sup> The results presented in this paper (and the observations from many other studies referred to above) are clearly commensurate with this mechanism, since prompt  $\text{Cl}_2$  emission is observed at temperatures in excess of 155 K. Furthermore, many different experimental techniques have shown that the reactive sticking probability of  $\text{ClONO}_2$  on HCl-doped ice falls rapidly as the surface becomes depleted of HCl ( $\text{Cl}^-$ ) and poisoned by the newly formed nitric acid hydrates. It is this effect that gives rise to the saturation behavior presented in Figure 14. These nitric acid hydrates are sufficiently well bound to their solvation shell to prevent the hydrolysis of further  $\text{ClONO}_2$  (in accordance with established reaction rates for the hydrolysis of  $\text{ClONO}_2$  on NAT-mimics with varying amounts of water<sup>83–86</sup>), while the lack of  $\text{Cl}^-$  prevents direct reaction. This kind of behavior is also observed when  $\text{ClONO}_2$  sticks to deliquescent NaCl aerosols, showing saturation as the available chloride ions are used up.<sup>87</sup> From a thermodynamic point of view, the energetics of attachment of both Cl atoms and  $\text{Cl}^-$  to  $\text{ClONO}_2$  in gas-phase studies are also favorable to this direct reaction mechanism.<sup>88,89</sup> Adsorption of  $\text{ClONO}_2$  (albeit transient) appears to permit Cl–O bond polarization in the water-rich environment of the surface and to thereby facilitate reaction with neighboring  $\text{Cl}^-$  ions.

## Conclusions

This work demonstrates that the heterogeneous reactions of HCl, HOCl, and  $\text{ClONO}_2$  are dominated not only by the reactive sticking of each reagent but also by the effects of adsorption and desorption at low temperatures. At realistic stratospheric temperatures and partial pressures, copious amounts of water are available to ensure that the reactions almost always occur on water-rich surfaces. It seems unlikely that any HOCl formed in the heterogeneous hydrolysis of  $\text{ClONO}_2$  will remain upon an ice particle surface for any appreciable period of time with the consequence that the direct reaction between HOCl and hydrates of HCl is only likely to occur if either impinging gaseous HOCl can react with adsorbed  $\text{H}_3\text{O}^+(\text{H}_2\text{O})_n\text{Cl}^-$ , which flow tubes studies suggest to be the case, or  $\text{H}_3\text{O}^+(\text{H}_2\text{O})_n\text{Cl}^-$  is available close to the site of impact of an incoming  $\text{ClONO}_2$  molecule. However, in the latter case, it is more probable that a direct reaction between  $\text{ClONO}_2$  and an adsorbed  $\text{Cl}^-$  ion will occur, releasing  $\text{Cl}_2$  directly. When all of the available chloride ions are used up or if the surface has been poisoned by the presence of reaction products such as nitrate ions, which hold on very strongly to their solvation shell, surface reactions will stop. In the real atmosphere, however, the situation may be completely different. The rapid condensation of fresh water<sup>90</sup> will serve to purify the surface and the adsorption of further

HCl (both  $\text{H}_2\text{O}$  and HCl achieve significant concentrations in the cold polar stratosphere) will produce new reaction sites. Further perturbation may occur because of surface-to-bulk diffusion. At these low temperatures, the diffusion of the reaction products into the bulk is not likely to be rapid. However, at 200 K, there is likely to be significant mobility. This may affect the ability of the surface to clean itself by for example removing nitrate ions into the bulk and also to replace HCl and water at the surface from the bulk. The rates of diffusion as a function of temperature and substrate composition are not well quantified for any of the materials described here. When the substrate is sulfuric acid, a rather different set of reactions may occur. Recent work by Donaldson et al.<sup>71</sup> has explored the detailed chemistry that can occur when strong acids (capable of protonating HOCl) are present, suggesting that the formation of the  $[\text{H}_2\text{OCl}^+]$  ion may participate in the heterogeneous chemistry of HOCl in and on sulfuric acid particles.<sup>71</sup> This may extend the lifetime of this species and enable it to react directly with species other than water. This may entirely change the product branching ratios of surface reactions and enable reactions to occur both on and within particles. The rate of transfer from the surface to the bulk, combined with the rate coefficients for the reactions (quantified in the form of the reactodiffusive length<sup>25</sup>) may enable accurate prediction of the effect and importance of internal and external reactions in various parts of the atmosphere.

What is clear from this and other mechanistic studies of heterogeneous stratospheric reactions is that particle surface composition, strongly influenced by ambient partial pressures, temperature, and relative humidity, is fundamental in determining the reaction pathways that lead to the generation of ozone-depleting species. A transition between particle compositions clearly engenders different reactivities and chemistry, since in water-rich, low-temperature conditions, hydrolysis will prevail, while higher temperatures will favor direct hydrated-ion reactions. The investigation of such mechanistic effects upon other species of interest such as  $\text{BrONO}_2$ , HOBr, BrCl, and HBr is required for deeper understanding. Similarly, the tendency of atmospheric species toward partial ionization upon adsorption at the temperatures prevalent in the atmosphere remains relatively unexplored, but may be paramount in determining the efficiency of many important reactions.

**Acknowledgment.** The authors would like to thank the NERC Laboratory Studies in Atmospheric Chemistry program and the CEC Environment program for financial assistance. We are grateful to the CEC for a research assistantship (N.A.W.) and to the EPSRC for a graduate studentship (T.B.R.). We would also like to thank Heather Donsig, Dawn Herridge, and John Vickerman for making their experimental results available to us prior to publication.

## References and Notes

- (1) Molina, M. J. *Angew. Chem., Int. Ed. Engl.* **1996**, *35*, 1778. Portman, R. W.; Solomon, S.; Garcia, R. R.; Thomason, L. W.; Poole, L. R. *J. Geophys. Res.* **1996**, *101*, 22991.
- (2) Harris, N. R. P.; Anvellet, G.; Bishop, L.; Hofmann, D. J.; Kerr, J. B.; McPeters, R. D.; Prende, M.; Randel, W. J.; Staehelin, J.; Subbaraya, B. H.; Volz-Thomas, A.; Zawodny, J.; Zerefos, C. S. *J. Geophys. Res.* **1997**, *102*, 1571.
- (3) Hofmann, D. J.; Oltmans, S. J.; Komhyr, W. D.; Harris, J. M.; Lathrop, J. A.; Langford, A. O.; Deshler, T.; Johnson, B. J.; Torres, A.; Matthews, W. A. *Geophys. Res. Lett.* **1994**, *21*, 65.
- (4) Elliott, S.; Cicerone, R. J.; Turco, R. P.; Drdla, K.; Tabazadeh, A. *J. Geophys. Res.* **1994**, *99*, 3497.
- (5) Drdla, K.; Turco, R. P.; Elliott, S. *J. Geophys. Res.* **1993**, *98*, 8965.

- (6) Gao, R. S.; Fahey, D. W.; Salawitch, R. J.; Lloyd, S. A.; Anderson, D. E.; DeMaijstre, R.; McElroy, C. T.; Woodbridge, E. L.; Wamsley, R. C.; Donnelly, S. G.; DelNegro, L. A.; Proffitt, M. H.; Stimpfle, R. M.; Kohn, D. W.; Kawa, S. R.; Lait, L. R.; Loewenstein, M.; Podolske, J. R.; Keim, E. R.; Dye, J. E.; Wilson, J. C.; Chan, K. R. *J. Geophys. Res.* **1997**, *102*, 3935.
- (7) Prather, M. J.; *Nature* **1992**, *355*, 534.
- (8) Pitari, G.; *Geophys. Res. Lett.* **1993**, *20*, 2663.
- (9) Dye, J. E.; Baumgardner, D.; Gandrud, B. W.; Kawa, S. R.; Kelly, K. K.; Loewenstein, M.; Ferry, G. V.; Chan, K. R.; Gary, B. L. *J. Geophys. Res.* **1992**, *97*, 8015.
- (10) Beyerle, G.; Neuber, R.; Schrems, O.; Wittrock, F.; Knudsen, B. *Geophys. Res. Lett.* **1994**, *21*, 57.
- (11) Grainger, R. G.; Lambert, A.; Rodgers, C. D.; Taylor, F. W.; Deshler, T. *J. Geophys. Res.* **1995**, *100*, 16507.
- (12) Turco, R. P.; Hamill, P. *Ber. Bunsen-Ges. Phys. Chem.* **1992**, *96*, 323.
- (13) Luo, B. P.; Clegg, S. L.; Peter, Th.; Muller, R.; Crutzen, P. J. *Geophys. Res. Lett.* **1994**, *21*, 49.
- (14) Carlsaw, K. S.; Luo, B. P.; Clegg, S. L.; Peter, Th.; Brimblecombe, P.; Crutzen, P. J. *Geophys. Res. Lett.* **1994**, *21*, 2479.
- (15) Song, N. *Geophys. Res. Lett.* **1994**, *21*, 2709.
- (16) Tabazadeh, A.; Toon, O. B.; Hamill, P. *Geophys. Res. Lett.* **1995**, *22*, 1725.
- (17) Koop, T.; Luo, B. P.; Biermann, U. M.; Crutzen, P. J.; Peter, Th. *J. Phys. Chem.* **1997**, *101*, 1117.
- (18) Rinsland, C. P.; Gunson, M. R.; Abrams, M. C.; Zander, R.; Mahieu, E.; Goldman, A.; Ko, M. K. W.; Rodriguez, J. M.; Sze, N. D. *J. Geophys. Res.* **1994**, *99*, 18895.
- (19) Chu, L. T.; Leu, M.-T.; Keyser, L. F. *J. Phys. Chem.* **1993**, *97*, 7779.
- (20) Hanson, D. R.; Ravishankara, A. R. *J. Phys. Chem.* **1993**, *97*, 12309.
- (21) Abbatt, J. P. D. *J. Geophys. Res.* **1995**, *100*, 14009.
- (22) Hanson, D. R.; Lovejoy, E. R. *J. Phys. Chem.* **1996**, *100*, 6397.
- (23) Fenter, F. F.; Caloz, F.; Rossi, M. J. *J. Phys. Chem.* **1996**, *100*, 1008.
- (24) Beichert, P.; Findlayson-Pitts, B. J. *J. Phys. Chem.* **1996**, *100*, 15218.
- (25) Hanson, D. R.; Ravishankara, A. R.; Solomon, S. *J. Geophys. Res.* **1994**, *99*, 3615.
- (26) Barton, N.; Rowland, B.; Devlin, J. P. *J. Phys. Chem.* **1993**, *97*, 5848.
- (27) Fried, A.; Henry, B. E.; Calvert, J. G.; Mozurkewich, M. *J. Geophys. Res.* **1994**, *99*, 3517.
- (28) Hu, J. H.; Abbatt, J. P. D. *J. Phys. Chem.* **1997**, *101*, 871.
- (29) Behnke, W.; George, C.; Scheer, V.; Zetsch, C. *J. Geophys. Res.* **1997**, *102*, 3795.
- (30) Ahmed, M.; Apps, C. J.; Hughes, C.; Watt, N. E.; Whitehead, J. C. *J. Phys. Chem.* **1997**, *101*, 1250.
- (31) Tolbert, M. A.; Middlebrook, A. M. *J. Geophys. Res.* **1990**, *95*, 22423.
- (32) Tolbert, M. A.; Koehler, B. G.; Middlebrook, A. M. *Spectrochim. Acta* **1992**, *48*, 1303.
- (33) Peil, S.; Schrems, O.; *Proc. SPIE* **1993**, *158*, 2089.
- (34) Zhang, R.; Leu, M.-T.; Keyser, L. F. *J. Geophys. Res.* **1995**, *100*, 18845.
- (35) Iraci, L. T.; Middlebrook, A. M.; Tolbert, M. A. *J. Geophys. Res.* **1995**, *100*, 20969.
- (36) Toon, O. B.; Tolbert, M. A.; Koehler, B. G.; Middlebrook, A. M.; Jordan, J. *J. Geophys. Res.* **1994**, *99*, 25631.
- (37) Middlebrook, A. M.; Berland, B. S.; George, S. M.; Tolbert, M. A.; Toon, O. B. *J. Geophys. Res.* **1994**, *99*, 25655.
- (38) Clapp, M. L.; Miller, R. E.; Worsnop, D. R. *J. Phys. Chem.* **1995**, *99*, 6317.
- (39) Anthony, S. E.; Tisdale, R. T.; Disselkamp, R. S.; Tolbert, M. A.; Wilson, J. C. *Geophys. Res. Lett.* **1995**, *22*, 1105.
- (40) Richwine, L. J.; Clapp, M. L.; Miller, R. E.; Worsnop, D. R. *Geophys. Res. Lett.* **1995**, *22*, 2625.
- (41) Clapp, M. L.; Niedziela, R. F.; Richwine, L. J.; Dransfield, T.; Miller, R. E.; Worsnop, D. R. *J. Geophys. Res.* **1997**, *102*, 8899.
- (42) Banham, S. F.; Horn, A. B.; Koch, T. G.; Sodeau, J. R. *Faraday Discuss.* **1995**, *100*, 321.
- (43) Koch, T. G.; Banham, S. F.; Sodeau, J. R.; Horn, A. B.; McCoustra, M. R. S.; Chesters, M. A. *J. Geophys. Res.* **1997**, *102*, 1513.
- (44) Hanson, D. R.; Ravishankara, A. R. *J. Geophys. Res.* **1991**, *96*, 5081.
- (45) Hanson, D. R.; Ravishankara, A. R. *J. Geophys. Res.* **1991**, *96*, 17307.
- (46) Hanson, D. R.; Ravishankara, A. R. *J. Phys. Chem.* **1992**, *96*, 2682.
- (47) Graham, J. D.; Roberts, J. T. *J. Phys. Chem.* **1994**, *98*, 5974.
- (48) Graham, J. D.; Roberts, J. T. *Geophys. Res. Lett.* **1995**, *22*, 251.
- (49) Horn, A. B.; Chesters, M. A.; McCoustra, M. R. S.; Sodeau, J. R. *J. Chem. Soc., Faraday Trans.* **1992**, *88*, 1077.
- (50) Abbatt, J. P. D.; Beyer, K. D.; Fucaloro, A. F.; McMahon, J. R.; Woodbridge, P. J.; Zhang, R.; Molina, M. J. *J. Geophys. Res.* **1992**, *97*, 15819.
- (51) Delzeit, L.; Rowland, B.; Devlin, J. P. *J. Phys. Chem.* **1993**, *97*, 10312.
- (52) Koehler, B. G.; McNeill, L. S.; Middlebrook, A. M.; Tolbert, M. A. *J. Geophys. Res.* **1993**, *98*, 10563.
- (53) Rieley, H.; Aslin, H. D.; Haq, S. *J. Chem. Soc., Faraday Trans.* **1995**, *91*, 2349.
- (54) Banham, S. F.; Sodeau, J. R.; Horn, A. B.; McCoustra, M. R. S.; Chesters, M. A. *J. Vac. Sci. Technol. A* **1996**, *14*, 1620.
- (55) Packer, M. J.; Clary, D. C. *J. Phys. Chem.* **1995**, *99*, 14323.
- (56) Wang, L. C.; Clary, D. C. *J. Chem. Phys.* **1996**, *104*, 5663.
- (57) Gertner, B. J.; Hynes, J. T. *Science* **1996**, *271*, 1563.
- (58) Foster, K. L.; Tolbert, M. A.; George, S. M. *J. Phys. Chem.* **1997**, *101*, 4979.
- (59) Oppliger, R.; Allanic, A.; Rossi, M. J. *J. Phys. Chem.* **1997**, *101*, 1903.
- (60) Collier, W. B.; Ritzhaupt, G.; Devlin, J. P. *J. Phys. Chem.*, **1984**, *88*, 363.
- (61) Woodbridge, P. J.; Devlin, J. P. *J. Chem. Phys.*, **1988**, *88*, 3086.
- (62) Horn, A. B.; Koch, T. G.; Chesters, M. A.; McCoustra, M. R. S.; Sodeau, J. R. *J. Phys. Chem.* **1994**, *98*, 946.
- (63) Koehler, B. G.; Middlebrook, A. M.; Tolbert, M. A. *J. Geophys. Res.* **1992**, *97*, 8065.
- (64) Guillory, W. A.; Bernstein, M. L. *J. Chem. Phys.* **1975**, *62*, 1058.
- (65) Koch, T. G.; Holmes, N. S.; Roddis, T. B.; Sodeau, J. R. *J. Phys. Chem.* **1996**, *100*, 11402.
- (66) Sodeau, J. R.; Horn, A. B.; Banham, S. F.; Koch, T. G. *J. Phys. Chem.* **1995**, *99*, 6258.
- (67) Gilbert, A. S.; Sheppard, N. *J. Chem. Soc., Faraday Trans. 2* **1973**, *67*, 1628. G. Ritzhaupt and J. P. Devlin, *J. Phys. Chem.*, **1991**, *95*, 90.
- (68) Horn, A. B.; Banham, S. F.; McCoustra, M. R. S. *J. Chem. Soc., Faraday Trans.* **1995**, *21*, 4005.
- (69) Kroes, G.-J.; Clary, D. C. *J. Phys. Chem.* **1992**, *96*, 7079.
- (70) Robinson Brown, A.; Doren, D. J. *J. Phys. Chem.* **1997**, *101*, 6308.
- (71) Donaldson, D. J.; Ravishankara, A. R.; Hanson, D. R. *J. Phys. Chem.* **1997**, *101*, 4717.
- (72) Atkins, P. W. *Physical Chemistry*, 5th ed.; Oxford University Press: Oxford, 1994.
- (73) Horn, A. B.; Sully, K. J. *J. Chem. Soc., Faraday Trans.* **1997**, *93*, 2741.
- (74) Bianco, R.; Hynes, J. T. *J. Phys. Chem. A* **1998**, *102*, 309.
- (75) Koch, T. G.; Horn, A. B.; Chesters, M. A.; McCoustra, M. R. S.; Sodeau, J. R. *J. Phys. Chem.* **1995**, *99*, 8362.
- (76) Hanson, D. R. *J. Phys. Chem.* **1995**, *99*, 13059.
- (77) La Manna, G. *J. Mol. Struct. (THEOCHEM)* **1994**, *309*, 31.
- (78) de Saxce, A.; Schriver, L. *Chem. Phys. Lett.* **1992**, *199*, 596.
- (79) Obermeyer, A.; Borrmann, H.; Simon, A. *J. Am. Chem. Soc.* **1995**, *117*, 7887.
- (80) Donsig, H. *Faraday Discuss.* **1995**, *100*, 333.
- (81) Donsig, H.; Herridge, D.; Vickerman, J. C. Submitted to *J. Phys. Chem.*
- (82) Donsig, H.; Herridge, D.; Vickerman, J. C. Personal communication.
- (83) Leu, M.-T.; Moore, S. B.; Keyser, L. F. *J. Phys. Chem.* **1991**, *95*, 7763.
- (84) Hanson, D. R.; Ravishankara, A. R. *J. Geophys. Res.* **1993**, *98*, 22931.
- (85) Abbatt, J. P. D.; Molina, M. J. *Geophys. Res. Lett.* **1992**, *19*, 461.
- (86) Abbatt, J. P. D.; Molina, M. J. *J. Phys. Chem.* **1992**, *96*, 7674.
- (87) Caloz, F.; Fenter, F. F.; Rossi, M. J. *J. Phys. Chem.* **1996**, *100*, 7494.
- (88) Haas, B.-M.; Crellin, K. C.; Kuwata, K. T.; Okumura, M. *J. Phys. Chem.* **1994**, *98*, 6470.
- (89) Yokelson, R. J.; Burkholder, J. B.; Goldfarb, L.; Fox, R. W.; Gilles, M. K.; Ravishankara, A. R. *J. Phys. Chem.* **1995**, *99*, 13976.
- (90) Haynes, D. R.; Tro, N. J.; George, S. M. *J. Phys. Chem.* **1992**, *96*, 8502.
- (91) Koch, T. G.; Holmes, N. S.; Roddis, T. B.; Sodeau, J. R., *J. Phys. Chem.* **1996**, *100*, 11402.
- (92) Horn, A. B.; Williams, N. A.; Roddis, T. B.; Sodeau, J. R. *J. Chem. Soc., Faraday Trans.* **1998**, *94*, 1721.